Chapter I.10

Synchrotron radiation

Rasmus Ischebeck
Paul Scherrer Institut, Villigen, Switzerland

Electrons circulating in a storage ring emit *synchrotron radiation*. The spectrum of this powerful radiation spans from the far infrared to the X-rays. Synchrotron radiation has evolved from being a mere byproduct of particle acceleration to a powerful tool leveraged in diverse scientific and engineering fields. Indeed, synchrotrons are the most brilliant X-ray sources on Earth, and they find use in a wide range of fields in research. In this chapter, we will look at the generation of radiation of charged particles in an accelerator, at the influence of this on the beam dynamics, and on the physics behind applications of synchrotron radiation for research.

I.10.1 Introduction

It is difficult to overstate the importance of X-rays for medicine, research and industry. Already a few years after their discovery by Wilhelm Conrad Röntgen, their ability to penetrate matter established X-rays as an important diagnostics tool in medicine. Experiments with X-rays have come a long way since the inception of the first X-ray tubes. The short wavelength of X-rays allowed Rosalynd Franklin and Raymond Gosling to take diffraction images that would lead to the discovery of the structure of DNA. Today, X-ray diffraction is an indispensable tool in structural biology and in pharmaceutical research. Industrial applications of X-rays range from cargo inspection to sterilization and crack detection.

In addition to bremsstrahlung from X-ray tubes, scientists use *synchrotron radiation* generated by relativistic electrons in vacuum, as those are accelerated by magnetic fields. Initially perceived as a nuisance in the context of high-energy physics accelerators, synchrotron radiation emerged as a critical factor limiting the energy gain in circular electron accelerators. However, its unique characteristics—such as high brightness, broad spectrum covering from infrared to X-rays, and excellent collimation—have transformed it into an invaluable asset in areas ranging from material science to biology. In this chapter, we will encounter accelerators such as the Swiss Light Source (see Fig. I.10.1), that are built solely to generate X-rays.

Synchrotrons, as well as free electron lasers, supply users with X-ray beams of unsurpassed brillance, and they attract scientists from various research fields. This brillance is the figure of merit for many experiments using X-rays, and is defined as

$$\mathcal{B} = \frac{\dot{N}_\gamma}{4\pi^2 \sigma_x \sigma_y \sigma_{x'} \sigma_{y'} (0.1\%\mathrm{BW})}. \tag{I.10.1}$$

This chapter should be cited as: Synchrotron radiation, R. Ischebeck, DOI: 10.23730/CYRSP-2024-003.433, in: Proceedings of the Joint Universities Accelerator School (JUAS): Courses and exercises, E. Métral (ed.),
CERN Yellow Reports: School Proceedings, CERN-2024-003, DOI: 10.23730/CYRSP-2024-003, p. 433.

Fig. I.10.1: View of the Swiss Light Source, with the roof removed for maintenance. Source: PSI Bildarchiv.

Figure I.10.2 shows the development of the peak brilliance of X-ray sources during the last century. Scientists working in synchrotron radiation facilities have gotten accustomed to an extremely high flux, as well as an excellent stability of their X-ray source. The flux is controlled on the permille level, and the position stability is measured in micrometers.

Synchrotron radiation was first observed on April 24, 1947 by Herb Pollock, Robert Langmuir, Frank Elder, and Anatole Gurewitsch, when they saw a gleam of bluish-white light emerging from the transparent vacuum tube of their new 70 MeV electron synchrotron at General Electric's Research Laboratory in Schenectady, New York[1]. It was first considered a nuisance because it caused the particles to lose energy, but it was recognised in the 1960s as radiation with exceptional properties that overcame the shortcomings of X-ray tubes. Furthermore, it was discovered that the emission of radiation improved the emittance of the beams in electron storage rings, and additional series of dipole magnets were installed at the Cambridge Electron Accelerator (CEA) at Harvard University to provide additional damping of betatron and synchrotron oscillations.

The evolution of synchrotron sources has proceeded in four generations, where each new generation made use of unique new features in science and engineering to increase the coherent flux available to experiments:

- **First generation: 1050s to 1970s.** Those were accelerators initially designed for high-energy physics experiments; synchrotron radiation was a byproduct. They were a significant advance with respect to X-ray tubes, but by today's standards, they are characterized by a relatively low brightness and flux. Radiation is generated in bending magnets that are used to keep electrons on a circular path. Examples for this generation include SPEAR at Stanford Linear Accelerator Center in the U.S., and DORIS at DESY in Germany.

[1] Arguably, the observation of synchrotron radiation from the supernova explosion on July 4, 1054 in what we now call the Crab Nebula came earlier, see Exercise I.10.7.4.

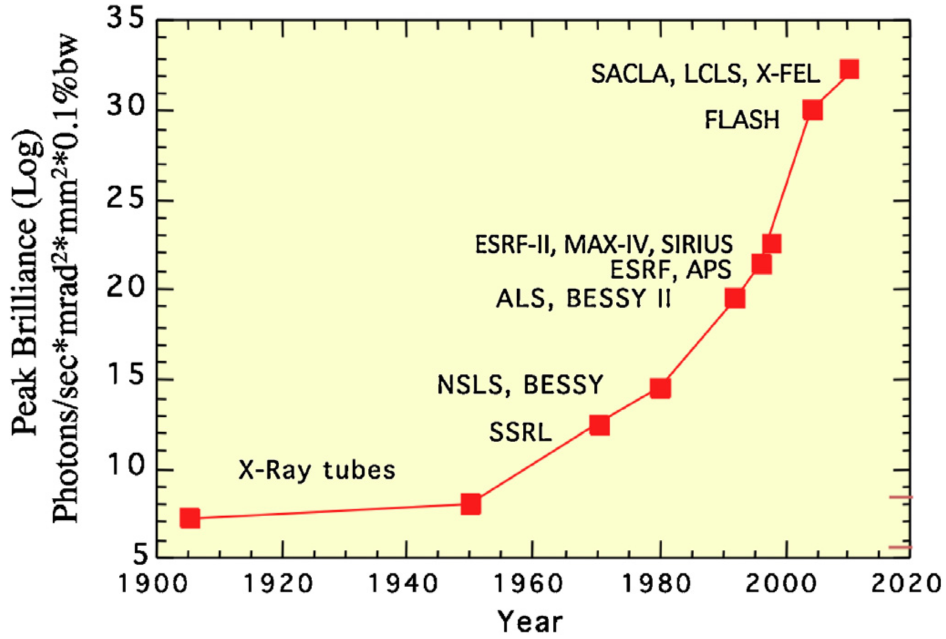

Fig. I.10.2: Development of peak brilliance of X-ray sources. Source: W. Eberhardt, Journal of Electron Spectroscopy and Related Phenomena 200 (2015) 31–39.

- **Second generation: Late 1970s to 1990s.** These accelerators were designed specifically as dedicated synchrotron radiation sources. Brightness and flux were increased with respect to the first generation, by utilizing wigglers to enhance the intensity of the emitted radiation. Their introduction broadened the applications in materials science, biology and chemistry. Examples include the National Synchrotron Light Source NSLS at Brookhaven National Laboratory in the U.S., and Aladdin at the University of Wisconsin-Madison, U.S.
- **Third generation: Early 1990s to present.** A major jump in brightness and flux, significantly surpassing earlier generations, was achieved by the introduction of undulators, where the particles radiate coherently at specific wavelengths in the forward direction. An enhanced beam stability was achieved by top-up injection schemes. Beamlines were optimized for specific techniques and applications, such as spectroscopy and diffraction for molecular biology. Examples include the European Synchrotron Radiation Facility ESRF in Grenoble, France, and the Advanced Photon Source APS at Argonne National Laboratory in the U.S.
- **Fourth generation: From the 2010s onwards.** Also known as *diffraction limited storage rings* (DLSRs), these facilities feature significantly reduced horizontal emittance, increasing the coherent flux significantly. We will look at these in detail in Section I.10.4. Examples include MAX IV in Lund, Sweden, and the upcoming SLS 2.0 in Villigen, Switzerland.

Synchrotrons are the de-facto standard for research using coherent X-ray beams. They are operated by national or European research laboratories, who make them available to academic and industrial researchers. Synchrotrons are now supplemented by *free electron lasers* (FELs), which make use of a linear accelerator to generate ultrabright electron beams that radiate coherently in long undulators. FELs are treated in Chapter III.7.

The key properties of synchrotron radiation are:

- Broad spectrum available,
- High flux,
- High spectral brightness,
- High degree of transverse coherence,
- Polarization can be controlled,
- Pulsed time structure,
- Stability,
- Power can be computed from first principles.

We will now navigate through the electromagnetic theory to understand how synchrotron radiation is generated when relativistic electrons are subjected to magnetic fields, noting in particular undulators, insertion devices present in every synchrotron radiation source. We will then look at the effect of the emission of synchrotron radiation on the particle bunches in a storage ring, and come to the surprising conclusion that this actually improves the emittance of the beam. We will then explore recent technological advancements in accelerator physics, which allow improving the transverse coherence of the X-ray beams significantly. Finally, we will look at the interaction of X-rays with matter, and give an overview of scientific uses of synchrotron radiation.

I.10.2 Generation of radiation by charged particles

An accelerated charge emits electromagnetic radiation. An oscillating charge emits radiation at the oscillation frequency, and a charged particle moving on a circular orbit radiates at the revolution frequency. As soon as the particles approach the speed of light, however, this radiation is shifted towards higher frequencies, and it is concentrated in a forward cone, as shown in Fig. I.10.3.

I.10.2.1 Non-relativistic particles moving in a dipole field

Let us first look at non-relativistic particles. In a constant magnetic field with magnitude B, a particle with charge e and momentum $p = mv$ will move on a circular orbit with radius ρ

$$\rho = \frac{p}{eB}.$$

This is an accelerated motion, and the particle emits radiation. For non-relativistic particles, this radiation is called *cyclotron radiation*, and the total emitted power is

$$P = \sigma_t \frac{B^2 v^2}{\mu_0 c}, \tag{I.10.2}$$

where σ_t is the Thomson cross section

$$\sigma_t = \frac{8\pi}{3} \left(\frac{e^2}{4\pi\varepsilon_0 mc^2} \right)^2. \tag{I.10.3}$$

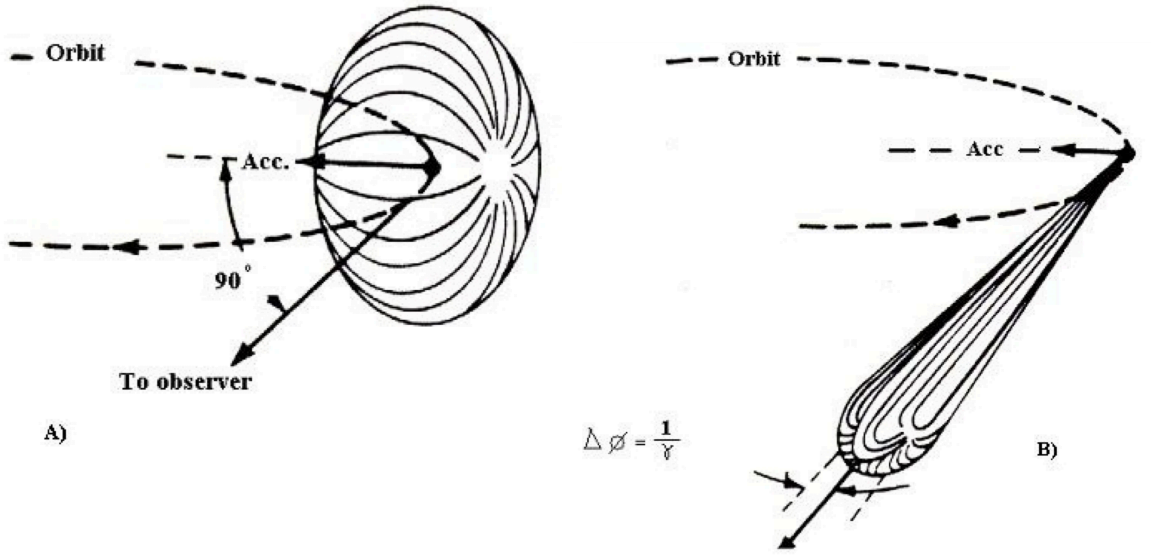

Fig. I.10.3: Emission of radiation from an accelerated particle: A) a non-relativistic particle moving on a circular orbit, B) a relativistic particle. Source: D. H. Tomboulian and P. L. Hartman, Phys. Rev. 102 (1956).

The radiation is emitted in all directions except in the direction of acceleration (see Fig. I.10.3 A). The frequency of the emitted radiation is exactly the revolution frequency

$$f = \frac{v}{2\pi\rho}.$$

I.10.2.2 Relativistic particles moving in a dipole field

For relativistic particles, this radiation is Lorentz-boosted in the forward direction (see Fig. I.10.3 B). The relativistic Doppler shift results in significantly shorter wavelengths, corresponding to higher photon energies. Furthermore, the radiation seen by an observer in the plane of revolution is pulsed, peaking every time that the particle passes by.

The properties of this so-called *synchrotron radiation* can be calculated directly from Maxwell's equations, without the need for material constants. For a particle that follows a trajectory $\vec{x} = \vec{r}(t)$, the charge density and the current distribution are given by

$$\rho(\vec{x}, t) = e\delta^{(3)}(\vec{x} - \vec{r}(t)) \quad \text{and} \quad \vec{j}(\vec{x}, t) = e\vec{v}(t)\delta^{(3)}(\vec{x} - \vec{r}(t)),$$

respectively. The solution to Maxwell's equations for this time-varying charge and current density can be found by using the wave equation for the electromagnetic potentials. In the Lorentz gauge, this wave equation reads

$$\vec{\nabla}^2\Phi - \frac{1}{c^2}\frac{\partial^2\Phi}{\partial t^2} = -\frac{e}{\varepsilon_0} \quad \vec{\nabla}^2\vec{A} - \frac{1}{c^2}\frac{\partial^2\vec{A}}{\partial t^2} = -\mu_0\vec{j}.$$

The general solutions for the potentials given by time-varying charge and current densities can be found by integrating over time and space

$$\Phi(\vec{x},t) = \frac{1}{4\pi\varepsilon_0}\int d^3\vec{x}'\int dt'\frac{\rho(\vec{x}',t)}{|\vec{x}-\vec{x}'|}\delta\left(t'+\frac{\vec{x}-\vec{x}'}{c}-t\right)$$

and

$$\vec{A}(\vec{x},t) = \frac{1}{4\pi\varepsilon_0 C^2}\int d^3\vec{x}'\int dt'\frac{\vec{j}(\vec{x}',t)}{|\vec{x}-\vec{x}'|}\delta\left(t'+\frac{\vec{x}-\vec{x}'}{c}-t\right).$$

Solving the wave equation in this most general sense is quite elaborate. The derivation can be found in Jackson [1], Chapter 6. Here, we just cite the result: the intensity of the radiation per solid angle $d\Omega$ and per frequency interval $d\omega$ is given by

$$\frac{d^3I}{d\Omega d\omega} = \frac{e^2}{16\pi^3\varepsilon_0 c}\left(\frac{2\omega\rho}{3c\gamma^2}\right)^2\left(1+\gamma^2\vartheta^2\right)^2\left[K_{2/3}^2(\xi)+\frac{\gamma^2\vartheta^2}{1+\gamma^2\vartheta^2}K_{1/3}^2(\xi)\right], \tag{I.10.4}$$

where K is the modified Bessel function of the second kind, γ is the relativistic factor of the particle, ϑ is the angle between the (local) trajectory of the particle and the observation point, and the normalized frequency ξ is given by

$$\xi = \frac{\omega\rho}{3c\gamma^3}\left(1+\gamma^2\vartheta^2\right)^{3/2}.$$

Due to the properties of the modified Bessel function, the radiation intensity is negligible for $\xi \gg 1$. We define the *critical frequency* ω_c as

$$\omega_c = \frac{3}{2}\frac{c}{\rho}\gamma^3. \tag{I.10.5}$$

The critical frequency is the typical frequency of synchrotron radiation: half of the energy is radiated at frequencies $\omega > \omega_c$, half at frequencies $\omega < \omega_c$. Correspondingly, we define a critical (i.e. a typical) photon energy E_c

$$E_c = \hbar\omega_c = \frac{3}{2}\frac{\hbar c}{\rho}\gamma^3. \tag{I.10.6}$$

The *critical angle* is defined as

$$\vartheta_c = \frac{1}{\gamma}\left(\frac{\omega_c}{\omega}\right)^{1/3}. \tag{I.10.7}$$

Higher frequencies have a smaller critical angle. For frequencies much larger than the critical frequency, and for angles much larger than the critical angle, the synchrotron radiation emission is negligible.

The total spectrum, integrated over all emission angles, is given by

$$\frac{dI}{d\omega} = \iint_{4\pi}\frac{d^3I}{d\omega d\Omega}d\Omega = \frac{\sqrt{3}e^2}{4\pi\varepsilon_0 c}\gamma\frac{\omega}{\omega_c}\int_{\omega/\omega_c}^{\infty}K_{5/3}(x)dx. \tag{I.10.8}$$

It is shown in Fig. I.10.4. Unlike cyclotron radiation, emitted by non-relativistic electrons, synchrotron radiation has a broadband spectrum, shifted towards higher photon energies with the cube of the Lorentz factor γ. In the Swiss Light Source, the Lorentz factor γ is approximately 5000. As a result, the critical frequency of the radiation emitted by the dipole magnets is in the exahertz range, corresponding to the X-ray spectrum. The overall spectrum of synchrotron radiation covers infrared, visible, UV and X-ray wavelengths. While coherent beams in or near the visible spectrum can be conveniently generated by lasers, synchrotrons are widely used in research that requires X-ray photons. We will look at some typical applications in Section I.10.6.

The total radiated power per particle, obtained by integrating over the spectrum, is

$$P_\gamma = \frac{e^2 c}{6\pi\varepsilon_0}\frac{\beta^4\gamma^4}{\rho^2}. \tag{I.10.9}$$

The energy lost by a particle on a circular orbit, i.e. in an accelerator consisting only of dipole magnets, is

$$U_0 = \frac{e^2\beta^4\gamma^4}{3\varepsilon_0\rho}, \tag{I.10.10}$$

where we have used $T = 2\pi\rho/c$, assuming $v \approx c$. Of course, real accelerators contain also other types of magnets. The energy lost per turn for a particle in an arbitrary accelerator lattice can be calculated by the following ring integral

$$U_0 = \frac{C_\gamma}{2\pi}E_{\text{nom}}^4 \oint \frac{1}{\rho^2}ds, \tag{I.10.11}$$

where E_{nom} is the nominal beam energy and

$$C_\gamma = \frac{e^2}{3\varepsilon_0(m_e c^2)^4}.$$

We define the following integral as the *second synchrotron radiation integral*

$$I_2 := \oint \frac{1}{\rho^2}ds. \tag{I.10.12}$$

From the energy lost per turn U_0 and the critical photon energy E_c, we can calculate an average number of photons to be approximately

$$\langle n_\gamma \rangle \approx \frac{16\pi}{9}\alpha_{\text{fine}}\gamma,$$

where $\alpha_{\text{fine}} \approx 1/137$ is the fine structure constant. This is a relatively small number; we will therefore have to consider the quantum nature of the radiation, and we will see later how this quantum nature ultimately defines the beam emittance in an electron storage ring.

The total radiated power depends on the fourth power of the Lorentz factor γ, or for a given particle energy, it is inversely proportional to the fourth power of the mass of this particle. This means that synchrotron radiation, and its effect on the beam, are negligible for all proton accelerators except for the highest-energy one. For electron storage rings, conversely, this radiation dominates power losses of the beam, the evolution of the emittance in the ring, and therefore the beam dynamics of the accelerator. Before we will look at this in detail, we will treat one particular case where the electrons pass through a sinusoidal magnetic field. Such a field, generated by wigglers and undulators[2], gives rise to strong radiation in the forward direction, which makes it particularly useful for applications of X-rays.

[2]Historically, one distinguished *wigglers* and *undulators*, depending on the so-called undulator parameter $K = e/(2\pi m_e c) \cdot B_0 \cdot \lambda_U$ (where B_0 is the field on axis and λ_U is the undulator period). Wigglers ($K > 1$) used strong magnets and long periods, resulting in an orbit that deviates significantly from a straight line. They basically consisted of several dipole magnets in a row, such that the field would add up. Undulators ($K < 1$), conversely, are high-precision devices that resulted in small deviations of the particle trajectories from a straight line, such that the radiation from subsequent periods adds up coherently. Today, precision manufacturing methods allow to control the orbit precisely even for $K > 1$, thus the distinction between wigglers and undulators is less clear, and these devices are commonly refered to as insertion devices.

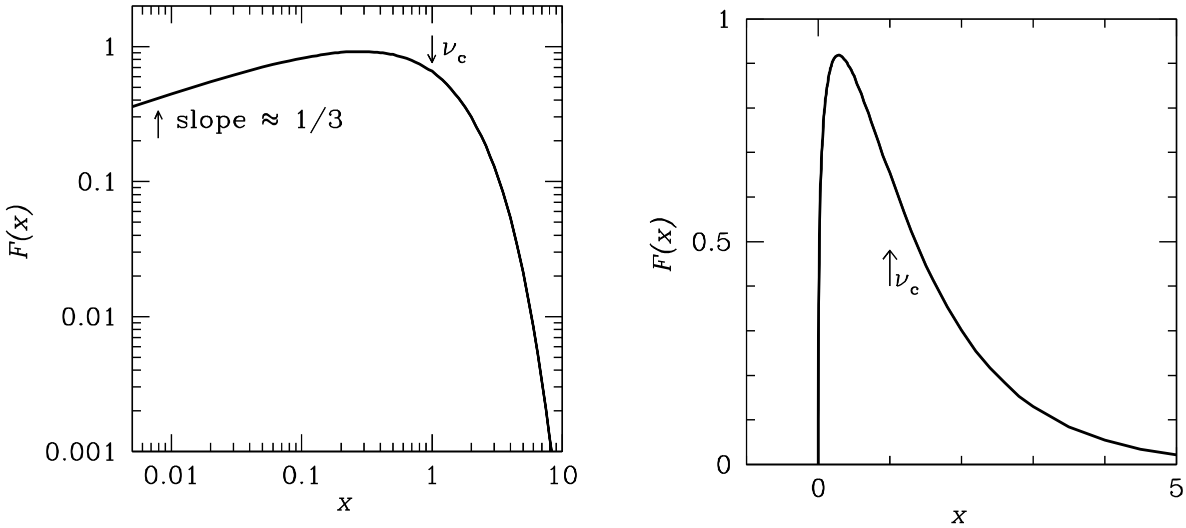

Fig. I.10.4: Spectrum of synchrotron radiation, shown on logarithmic axes (left) and on a linear scale (right). The horizontal axis shows the frequency, relative to the critical frequency ($x = 1$ corresponds to $\nu = \nu_c$.) The vertical axis shows the spectral flux. Source: https://www.cv.nrao.edu/course/astr534/SynchrotronSpectrum.html.

I.10.2.3 Coherent generation of X-rays in undulators

Wiggler and undulator magnets are devices that impose a periodic magnetic field on the electron beam. These insertion devices have been specially designed to excite the emission of electromagnetic radiation in particle accelerators.

Let us assume a cartesian coordinate system with an electron travelling in z direction.

A planar insertion device, with a mangetic field in the vertical direction y, has the following field on axis

$$\vec{B}(0, 0, z) = \vec{u}_y B_0 \sin(k_u z), \tag{I.10.13}$$

where $k_u = 2\pi/\lambda_u$ with λ_u the period of the magnetic field, B_0 is the maximum field and $\vec{u}_y$ is the unit vector in y direction. Due to the *Maxwell* equations, the curl and divergence of the static magnetic field vanish in vacuum, $\vec{\nabla} \times \vec{B} = 0$ and $\vec{\nabla} \cdot \vec{B} = 0$. Thus, the field acquires a z component for $y \neq 0$

$$\begin{aligned} B_x &= 0 \\ B_y &= B_0 \cosh(k_u y) \sin(k_u z) \\ B_z &= B_0 \sinh(k_u y) \cos(k_u z). \end{aligned}$$

The difference to Equation I.10.13 is small for $k_u y \ll 1$ and will be neglected in the following.

Helical undulators have a magnetic field on the axis

$$\vec{B}(z) = \vec{u}_x B_0 \cos(k_u z) - \vec{u}_y B_0 \sin(k_u z).$$

A rigorous analytic discussion of helical undulators is somewhat easier since the longitudinal component of the electron velocity $v_z = \beta_z c$ is constant. Planar undulators, however, are much more common in synchrotron radiation facilities, therefore we will continue our discussion using a magnetic field according to Equation I.10.13.

The magnetic field exerts a force on the electron

$$m_e\gamma\frac{\mathrm{d}\vec{v}}{\mathrm{d}t}=\vec{F}=-e\vec{v}\times\vec{B}$$

that results in a transverse oscillation of the particle

$$m_e\gamma\frac{\mathrm{d}v_x}{\mathrm{d}t}=ev_zB_y=ev_zB_0\sin(k_uz).$$

In the following, we replace the independent variable t by the longitudinal position z. Thus, the equation can be written as a derivative with respect to z, using $\mathrm{d}z/\mathrm{d}t=v_z$

$$\frac{\mathrm{d}v_x}{\mathrm{d}z}=\frac{e}{m_e\gamma}B_0\sin(k_uz).$$

The relativistic γ-factor of a particle is constant in a static magnetic field. Integration of the equation leads to

$$v_x(z)=\beta_z(z)c=-\frac{Kc}{\gamma}\cos(k_uz),\tag{I.10.14}$$

where a dimensionless undulator parameter has been introduced,

$$K=\frac{eB_0}{m_eck_u}.\tag{I.10.15}$$

The electron follows a sinusoidal trajectory

$$x(z)=-\frac{K}{k_u\gamma\beta_z}\sin(k_uz).$$

Synchrotron radiation is emitted by relativistic electrons in a cone with opening angle of approximately $\frac{1}{\gamma}$ (Equation I.10.7). In an *undulator*, the maximum angle of the particle velocity with respect to the undulator axis $\alpha=\arctan(\frac{v_x}{v_z})$ is always smaller than the opening angle of the radiation, therefore the radiation field may add coherently.

Consider two photons emitted by a single electron at the points A and B, which are one half undulator period apart (see Fig. I.10.5)

$$\overline{AB}=\frac{\lambda_u}{2}.$$

If the phase of the radiation wave advances by π between A and B, the electromagnetic field of the radiation adds coherently[3]. The light moves on a straight line $\overline{AB}$ that is slightly shorter than the sinusoidal electron trajectory $\widetilde{AB}$

$$\frac{\lambda}{2c}=\frac{\widetilde{AB}}{v}-\frac{\overline{AB}}{c}.\tag{I.10.16}$$

[3]Photons radiated by different electrons will however usually be incoherent.

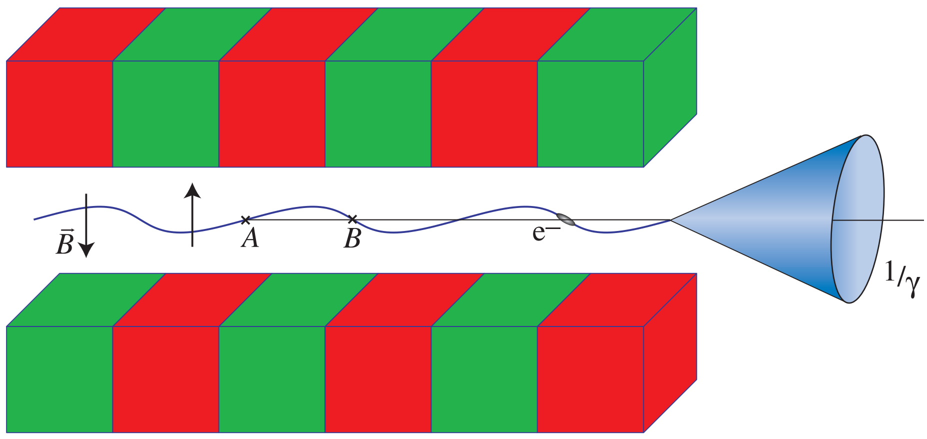

Fig. I.10.5: Emission of radiation in an undulator.

The electron travels on a sinusoidal arc of length $\widetilde{AB}$ that can be calculated as

$$\begin{aligned}
\widetilde{AB} &= \int_0^{\lambda_u/2} \sqrt{1+\left(\frac{\mathrm{d}x}{\mathrm{d}z}\right)^2}\,\mathrm{d}z \\
&\approx \int_0^{\lambda_u/2} \left(1+\frac{1}{2}\left(\frac{\mathrm{d}x}{\mathrm{d}z}\right)^2\right)\mathrm{d}z \\
&= \int_0^{\lambda_u/2} \left(1+\frac{K^2}{2\beta_z^2\gamma^2}\cos^2(k_u z)\right)\mathrm{d}z \\
&= \frac{\lambda_u}{2}\left(1+\frac{K^2}{4\beta_z^2\gamma^2}\right) \\
&\approx \frac{\lambda_u}{2}\left(1+\frac{K^2}{4\gamma^2}\right).
\end{aligned}$$

Equation (I.10.16) becomes

$$\begin{aligned}
\frac{\lambda}{2c} &= \frac{\lambda_u}{2\beta c}\left(1+\frac{K^2}{4\gamma^2}\right) - \frac{\lambda_u}{2c} \\
\Longrightarrow \quad \lambda &= \frac{\lambda_u}{2\gamma^2}(1+K^2/2), \qquad \text{(I.10.17)}
\end{aligned}$$

where we have used $\beta = \sqrt{1-\gamma^{-2}} \approx 1 - \frac{1}{2}\gamma^{-2}$ for $\gamma \gg 1$. Radiation emitted at this wavelength adds up coherently in the forward direction. More generally, the radiation adds up coherently at all odd harmonics $n = 2m-1, m \in \mathbb{N}$

$$\lambda_n = \frac{\lambda_u}{2n\gamma^2}\left(1+\frac{K^2}{2}\right), \qquad \text{(I.10.18)}$$

while we have destructive interference for even harmonics $n = 2m, m \in \mathbb{N}$. If we observe the radiation under a small angle ϑ from the beam axis, the emission is slightly red-shifted

$$\lambda = \frac{\lambda_u}{2\gamma^2}\left(1 + \frac{K^2}{2} + \vartheta^2\gamma^2\right). \tag{I.10.19}$$

As you can see, since $\vartheta^2\gamma^2 > 0$, the wavelength increases the further away from the axis it is observed. the angular width $\Delta\vartheta$ of the radiation cone is inversely proportional to the distance L traveled by the radiation: $\Delta\theta \propto \frac{1}{L}$. This occurs because the wavefronts from different points of the trajectory become more aligned the farther they travel, effectively narrowing the observed radiation cone.

Two important aspects:

- The photon energy is proportional to the square of the energy of the electrons;
- The photon energy decreases with higher magnetic field.[4]

We are looking at spontaneous radiation, thus the total energy loss of the electrons is proportional to the distance travelled. Consequently, the total intensity of the radiation grows proportionally to the distance travelled. The width of the radiation cone for the fundamental wavelength decreases inversely proportional to the distance, therefore the central intensity grows as the square of the undulator length. The radiation is linearly polarized in x direction.

Undulators thus make use of the coherent enhancement of the radiation of each electron individually, which leads to a substantial increase in brillance (Equation I.10.1). This coherence occurs at specific wavelengths, which can be tuned by adjusting the strength of the magnetic field[5], and occurs in a very narrow angle around the forward direction. Free electron lasers achieve an additional coherent enhancement from multiple electrons in each microbunch, which results in another supercalifragilistic-expialidocious enhancement in the peak brilliance.

To compute the brillance of the radiation from an undulator, one first has to determine the flux $\dot{N}_\gamma$ and the effective source size $\sigma_{(x,y)\text{eff}}$ and divergence $\sigma_{(x',y'),\text{eff}}$. These are given by the electron beam size $\sigma_{(x,y)}$ and divergence $\sigma_{(x',y')}$, and the diffraction limit for the radiation. Electron beam size and divergence can be calculated from the Twiss parameters β and γ, and the emittance ε of the beam. The diffraction limits for the radiation σ_r and $\sigma_{r'}$ can be calculated, considering the length of the source (which is equal to the undulator length) L

$$\sigma_r = \frac{1}{4\pi}\sqrt{\lambda L} \tag{I.10.20}$$

$$\sigma_{r'} = \sqrt{\frac{\lambda}{L}}. \tag{I.10.21}$$

This diffraction limit is symmetric in x and y. The effective source size is

$$\sigma_{(x,y),\text{eff}} = \sqrt{\sigma^2_{(x,y)} + \sigma^2_r} \tag{I.10.22}$$

[4]This appears somewhat unintuitive at first sight, as we have seen before that the critical photon energy is proportional to the magnetic field (Eq. I.10.6). In the present paragraph, we are looking at the photon energy at which *coherent emission* occurs, and indeed a higher magnetic field leads to a larger deviation from the straight line, resulting in a longer wavelength and thus a smaller photon energy.

[5]Conceptually, one could also tune the wavelength by adjusting the electron energy, but this is never done in synchrotrons.

$$\sigma_{(x',y'),\mathrm{eff}} \quad = \quad \sqrt{\sigma^2_{(x',y')} + \sigma^2_{r'}}. \tag{I.10.23}$$

Computing the photon flux $\dot{N}_\gamma$ for an undulator is even more elaborate than the calculation for a single dipole, and we just cite the result [2]

$$\dot{N}_\gamma = 1.43 \cdot 10^{14} N I_b Q_n(K), \tag{I.10.24}$$

where

$$Q_n(K) = \frac{1 + K^2/2}{n} F_n(K).$$

We denote the harmonic number by $n = 2m - 1$ with $m \in \mathbb{N}$, the number of periods in the undulator by N, the beam current in A by I_b, the undulator parameter by K, and $F_n(K)$ is given by

$$F_n(K) \quad = \quad \frac{n^2 K^2}{(1 + K^2/2)^2} \left(J_{(n+1)/2}(Y) - J_{(n-1)/2}(Y)\right)^2 \tag{I.10.25}$$

$$Y \quad = \quad \frac{nK^2}{4(1 + K^2/2)}, \tag{I.10.26}$$

where J is the Bessel function of the first kind.

As K increases, the higher harmonics play a more signicificant role, but the fundamental harmonic always has the highest flux.

I.10.3 Effects of the emission of radiation on beam dynamics

In this section, we will delve deeper into the interplay between the radiation emission and the ensuing dynamics of the beam. The treatment closely follows the book by Wolski [4]. First, we will explore the energy transfer that occurs when an electron emits a photon. Following this, we will make a coordinate transformation to the more beneficial action and angle variables, providing a clearer perspective on the underlying mechanisms. We will then proceed to compute the ensemble average to calculate the implications on the emittance of the beam. A noteworthy observation will emerge from our analysis: the emittance decreases exponentially, plateauing at a limit dictated by the fundamental principles of quantum mechanics. This revelation underscores the intricate ties between quantum mechanics and relativistic beam dynamics, shedding light on the broader consequences of radiation emission in storage rings.

In the following sections, we will make use of Hamiltonian mechanics. Those not familiar with this matter are invited to watch two introductory videos: "Hamiltonian formalism 1"[6] and "Hamiltonian formalism 2"[7].

I.10.3.1 Vertical damping

To begin, we will focus our attention on the vertical coordinate y; it turns out that this is the simplest case. We will look at one electron in the bunch, and choose the canonical variables y for position (measured

[6] https://youtu.be/6yb0kUQ1srE
[7] https://youtu.be/nm7f8XSGf7U

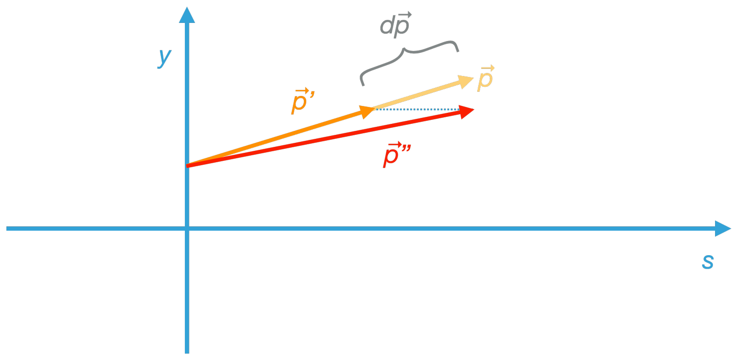

Fig. I.10.6: Illustration of the momentum change of a particle in a synchrotron, upon emission of a photon. The initial momentum is denoted by $\vec{p}$. After the emission of a photon with momentum $d\vec{p}$, the electron is left with a momentum $\vec{p'}$. Re-acceleration by the RF cavities replenishes the forward momentum of the particle, now denoted as $\vec{p''}$. From this illustration, it is intuitively clear that the transverse momentum is reduced. A mathematical derivation of the momentum change is given in the text.

relative to the reference orbit) and p_y to denote vertical momentum.

Let us consider an electron possessing a momentum p. Upon the emission of a photon with momentum dp, there is an associated change in momentum, which we will represent as $-dp$. As we have seen before, it is an intrinsic property of radiation emission by relativistic particles that it predominantly occurs in the forward direction. It is therefore a useful approximation to consider the momentum of the electron p and the emitted photon dp to be collinear. This collinearity is depicted in Fig. I.10.6.

The new momentum of the electron is then

$$\begin{aligned}\vec{p'} &= \vec{p} - d\vec{p} \\ &\approx \vec{p} - \frac{\vec{p}}{P_0}dp \\ &= \vec{p}\left(1 - \frac{d\vec{p}}{P_0}\right),\end{aligned}$$

where P_0 is the momentum of the reference particle. Since $\vec{p}$ and $d\vec{p}$ are collinear, the same relation can be written for the y component of $\vec{p}$, p_y

$$p'_y \approx p_y\left(1 - \frac{dp}{P_0}\right).$$

In order to analyze the effect on the beam, it becomes appropriate to transition to a more beneficial set of coordinates. Specifically, we will use the action and angle variables J_y and φ_y. It is essential to underscore that these coordinates are not arbitrary choices; they too are canonical variables. Their significance lies in their ability to offer a more structured view into the dynamics of the entire beam.

The action J_y is, by its definition

$$J_y = \frac{1}{2}\gamma_y y^2 + \alpha_y y p_y + \frac{1}{2}\beta_y p_y^2.$$

After the emission of a photon, the action of our single electron is

$$\begin{aligned}
J'_y &= \frac{1}{2}\gamma_y y^2 + \alpha_y y p_y \left(1 - \frac{dp}{P_0}\right) + \frac{1}{2}\beta_y p_y^2 \left(1 - \frac{dp}{P_0}\right)^2 \\
&= \frac{1}{2}\gamma_y y^2 + \alpha_y y p_y - \alpha_y y p_y \frac{dp}{P_0} + \frac{1}{2}\beta_y p_y^2 - 2 \cdot \frac{1}{2}\beta_y p_y^2 \frac{dp}{P_0} + \frac{1}{2}\beta p_y^2 \left(\frac{dp}{P_0}\right)^2 .
\end{aligned}$$

The change in action is thus

$$\begin{aligned}
dJ_y &= J'_y - J_y \\
&\approx -\alpha_y y p_y \frac{dp}{P_0} - \beta_y p_y^2 \frac{dp}{P_0} \\
&= -\left(\alpha_y y p_y + \beta_y p_y^2\right) \frac{dp}{P_0}.
\end{aligned}$$

Shifting our view to a broader perspective, we now consider the properties of the entire electron bunch. By definition, the emittance is given as the ensemble average of the action. The change in emittance follows thus from the change in action

$$\begin{aligned}
d\varepsilon_y &= \langle dJ_y \rangle \\
&= -(\alpha_y \underbrace{\langle y p_y \rangle}_{=-\alpha_y \varepsilon_y} + \beta_y \underbrace{\langle p_y^2 \rangle}_{=\gamma_y \varepsilon_y}) \frac{dp}{P_0} \\
&= -(-\alpha_y^2 \varepsilon_y + \beta_y \gamma_y \varepsilon_y) \frac{dp}{P_0} \\
&= -\varepsilon_y \underbrace{(\beta_y \gamma_y - \alpha_y^2)}_{1} \frac{dp}{P_0} \\
&= -\varepsilon_y \frac{dp}{P_0},
\end{aligned}$$

where we have used the Twiss parameter identity $\alpha_y^2 = \beta_y \gamma_y$. The change in emittance is thus proportional to the emittance, with a proportionality factor $-dp/P_0$. We thus have an exponentially decreasing emittance (the factor 2 is by convention)

$$\varepsilon_y(t) = \varepsilon_y(0) \cdot \exp\left(-2\frac{t}{\tau_y}\right). \tag{I.10.27}$$

This result underscores the value of the chosen variable transformation. By using action and angle variables, we can get an understanding of a key characteristic of the electron bunch: its emittance. This variable transformation is not just a mathematical maneuver; it serves as a powerful tool, offering clarity and depth to our exploration.

Note that we assume the momentum of the photon to be much smaller than the reference momentum. As a result, we see a slow (i.e. an adiabatic) damping of the emittance.

To proceed our determination of the vertical damping time, i.e. the decay constant of the emittance, we need to quantify the energy lost by a particle due to synchrotron radiation for each turn in the storage ring. We start with the radiation power

$$P_\gamma = \frac{C_\gamma}{2\pi} c \frac{E^4}{\rho^2}.$$

As the energy spread and the change in energy around one turn will be small, we can replace the particle energy E by the nominal energy E_{nom}.

The emission of synchrotron radiation leads to a decrease in the energy of the particles within a storage ring. In order to maintain these particles within the beam pipe, it is imperative to counterbalance this energy loss. This compensation is achieved using radio frequency (RF) cavities. These cavities are specifically designed to accelerate particles in the forward direction, ensuring their continued trajectory within the ring. The y component of the momentum is thus unchanged. In Fig. I.10.6, the momentum of a particle, after undergoing energy diminution due to radiation emission and subsequent re-acceleration by the RF cavities, is denoted as p''.

Let us get back to the change of emittance in one turn

$$d\varepsilon_y = -\varepsilon_y \frac{U_0}{E_{\text{nom}}}.$$

Using the revolution period T_0

$$\frac{d\varepsilon_y}{dt} = -\varepsilon_y \frac{U_0}{E_{\text{nom}} T_0}.$$

The damping time is thus

$$\tau_y = 2 \frac{E_{\text{nom}}}{U_0} T_0. \tag{I.10.28}$$

We use the (classical) result from Equation I.10.9 for the power radiated by a particle of charge e and energy E_{nom}. Integrating around the ring, we have the energy loss per turn

$$\begin{aligned} U_0 &= \oint P_\gamma dt \\ &= \oint \frac{1}{c} P_\gamma ds \\ &= \frac{C_\gamma}{2\pi} E_{\text{nom}}^4 \oint \frac{1}{\rho^2} ds. \end{aligned} \tag{I.10.29}$$

For a synchrotron consisting of only dipoles

$$\oint \frac{1}{\rho^2} ds = \frac{2\pi\rho}{\rho^2} = \frac{2\pi}{\rho}.$$

More generally, we use the second synchrotron radiation integral as defined in Equation I.10.12, and we can write the energy loss per turn as a function of I_2

$$U_0 = \frac{C_\gamma}{2\pi} E_{\text{nom}}^4 I_2. \tag{I.10.30}$$

Notice that I_2 is a property of the lattice (actually, a property of the reference trajectory), and does not depend on the properties of the beam.

The emittance evolves as

$$\varepsilon_y(t) = \varepsilon_y(0) \exp\left(-2\frac{t}{\tau_y}\right). \tag{I.10.31}$$

From this, it follows that the emittance decreases exponentially, asymptotically approaching zero. This phenomenon is termed *radiation damping*. While radiation damping plays a key role in influencing the emittance of the beam in a synchrotron, there exist other factors and effects that counterbalance its influence. These countering mechanisms ensure that the emittance does not perpetually decline due to the sole influence of radiation damping, but that it reaches a non-zero equilibrium value. Before diving into these balancing effects, we turn our attention to the horizontal plane, examining its unique characteristics and dynamics in the context of our ongoing analysis.

I.10.3.2 Horizontal damping

When considering the horizontal phase space (x, p_x), the situation is slightly more complicated. The primary factor contributing to this complexity is the dispersion, which introduces a coupling between the horizontal motion and the longitudinal phase space (z, δ). Notably, in regions where the reference trajectory is curved, such as within dipoles, the path length undertaken by a particle depends on its horizontal position relative to the reference trajectory. Further complicating matters, in accelerators where combined-function magnets are used, the dipole fields have a transverse gradient, thus the vertical magnetic field is influenced by its horizontal position.

The coupling between longitudinal and horizontal phase spaces in a beam is characterized by the dispersion $\eta_x = \partial x/\partial\delta$ and the dispersion derivative $\eta_{px} = \partial\eta_x/\partial z$. The canonic variables for the horizontal phase space are then given by

$$\begin{aligned} x &= \sqrt{2\beta_x J_x}\cos\varphi_x + \eta_x\delta \\ p_x &= -\sqrt{\frac{2J_x}{\beta_x}}(\sin\varphi_x + \alpha_x\cos\varphi_x) + \eta_{px}\delta. \end{aligned}$$

When deriving the equations for the beam dynamics in the horizontal phase space, we need to consider:

- **Change in momentum:** the emission of radiation leads to a recoil of the electron. This change in momentum is the same that we considered in the vertical phase space;
- **Dispersion:** the emission of radiation results in a change in the energy deviation, denoted as δ. This deviation brings about subsequent changes in the horizontal coordinate x and its associated momentum p_x.

When we explored the beam dynamics in the vertical phase space, we ignored the second factor, as we assumed that the vertical dispersion is zero. This assumption streamlined the analysis, but it can certainly not be made in the horizontal dimension.

While the details of the interplay between the emission of synchrotron radiation and the damping of the emittance are unique to each plane, the outcomes are similar. The horizontal emittance decays exponentially

$$\frac{d\varepsilon_x}{dt} = -\frac{2}{\tau_x}\varepsilon_x$$

$$\Rightarrow \varepsilon_x(t) = \varepsilon_x(0) \exp\left(-2\frac{t}{\tau_x}\right) \tag{I.10.32}$$

with a horizontal damping time

$$\tau_x = \frac{2}{j_x}\frac{E_0}{U_0}T_0. \tag{I.10.33}$$

All effects related to the dispersion are summarized in the horizontal partition number j_x

$$j_x = 1 - \frac{I_4}{I_2}. \tag{I.10.34}$$

The second synchrotron radiation integral is defined in Equation I.10.12. For the sake of completeness, we now define all five synchrotron radiation integrals

$$\begin{aligned}
I_1 &= \oint \frac{\eta_x}{\rho} ds \\
I_2 &= \oint \frac{1}{\rho^2} ds \\
I_3 &= \oint \frac{1}{|\rho|^3} ds \\
I_4 &= \oint \frac{\eta_x}{\rho}\left(\frac{1}{\rho^2} + 2k_1\right) ds, \qquad k_1 = \frac{e}{P_0}\frac{\partial B_y}{\partial x} \\
I_5 &= \oint \frac{\mathcal{H}_x}{|\rho|^3} ds, \qquad \mathcal{H}_x = \gamma_x \eta_x^2 + 2\alpha_x \eta_x \eta_{px} + \beta_x \eta_{px}^2.
\end{aligned} \tag{I.10.35}$$

All synchrotron radiation integrals are a function of the lattice, independent of the properties of the stored beam.

Again, Equation I.10.32 would predict an emittance that decays exponentially, approaching zero. The reason that this does not happen in reality is that there are effects that increase the horizontal emittance and thus result in a non-zero equilibrium emittance. We will soon look at these effects, but not before examining the longitudinal phase space.

I.10.3.3 Longitudinal damping

We will now look at the effect of synchrotron radiation on the longitudinal phase space (z, δ). Electrons that have a larger energy than the reference particle radiate more, while those that have smaller energy radiate less. This leads to a damping of the oscillations in the longitudinal phase space (the so-called *synchrotron oscillations*), and the longitudinal emittance, i.e. the phase space volume of the beam, decays exponentially.

This phase space is again coupled to the horizontal phase space, for the reasons mentioned above. Finding the damping time, one follows a derivation similar as in the vertical phase space:

- Write down the equations of motion of a single electron in the longitudinal phase space, including losses through synchrotron radiation;
- Express the energy loss per turn as a function of δ. The fact that this influences the radiation power introduces longitudinal damping;
- Note that the revolution period depends on the energy of the particle, with higher energy particles

taking longer for one turn[8];

- Solving the equations of motion gives synchrotron oscillations with an amplitude that decays exponentially;
- Finally, we take the ensemble average to find the longitudinal emittance.

This results in an exponentially decaying longitudinal emittance

$$\varepsilon_z(t) = \varepsilon_z(0) \exp\left(-2\frac{t}{\tau_z}\right), \tag{I.10.36}$$

with a damping time

$$\tau_z = \frac{2}{j_z}\frac{E_0}{U_0}T_0, \tag{I.10.37}$$

where the longitudinal damping partition number j_z is given by

$$j_z = 2 + \frac{I_4}{I_2}. \tag{I.10.38}$$

I.10.3.4 Quantum excitation

Finally, we are ready to look at effects that increase the emittance of the beam. While radiation damping inherently reduces emittance, there exist concurrent processes and phenomena that act in opposition, increasing the emittance. When such effects are integrated into our analysis, these emittance-increasing effects can counterbalance the radiation damping. As a consequence of this dynamic equilibrium between damping and amplifying factors, the beam stabilizes at a non-zero equilibrium emittance. This state represents a balance where the rate of emittance reduction due to radiation damping is compensated by the rate of emittance growth from other processes.

Let us first consider the horizontal phase space. An electron emitting an X-ray photon receives an equal and opposite recoil momentum. This quantized emission process is inherently stochastic, leading to fluctuations in the energy of individual electrons. As a consequence of these quantum fluctuations, the momentum change due to the emission of individual photons thus increases the horizontal emittance. The process is further amplified by the dispersion of the lattice.

Including the effects of radiation damping and quantum excitation, the emittance in the horizontal plane varies as

$$\varepsilon_x(t) = \varepsilon_x(0) \exp\left(-2\frac{t}{\tau_x}\right) + \varepsilon_x(\infty)\left[1 - \exp\left(-2\frac{t}{\tau_x}\right)\right] \tag{I.10.39}$$

and the equilibrium value, also called the *natural horizontal emittance* is

$$\varepsilon_x(\infty) = C_q\gamma^2\frac{I_5}{j_x I_2}, \tag{I.10.40}$$

where the fifth synchrotron radiation integral I_5 is defined in Equation I.10.35, and the electron quantum constant C_q is

$$C_q = \frac{55}{32\sqrt{3}}\frac{\hbar}{m_e c} \approx 3.832 \cdot 10^{-13}\,\mathrm{m}. \tag{I.10.41}$$

[8] Electrons are typically highly relativistic, such that synchrotrons are always above transition energy.

(The factor $\frac{55}{32\sqrt{3}}$ comes from the calculation of the emission spectrum of synchrotron radiation, integrating over all photon energies and angles).

A similar effect occurs in the longitudinal phase space. An electron emitting an X-ray photon loses a small, but significant fraction of its energy. This induces an energy spread among the electrons in the bunches. This energy spread, in tandem with the action of dispersion in the accelerator, results in an increase in the longitudinal phase space distribution, thereby increasing the longitudinal emittance of the beam. Quantum excitation thus acts as a natural counterpart to radiation damping.

The natural energy spread $\Delta E/E$ is given by

$$\frac{\Delta E}{E} = \sqrt{\frac{C_q \gamma^2}{2 j_z \langle \rho \rangle}}, \tag{I.10.42}$$

where $\langle \rho \rangle$ is the average radius of curvature in the storage ring.

Finally, in the vertical phase space of accelerators, the dynamics are somewhat different than in the horizontal or longitudinal phase spaces. This is primarily because of typically negligible dispersion in the vertical plane, and because this phase space is typically not coupled to the other dimensions. This means that, under normal conditions, variations in the energy of a particle do not significantly affect its vertical position. However, that does not exempt the vertical phase space from the effects of quantum excitation. Three effects remain that counterbalance radiation damping even in the vertical plane:

– A (small) vertical component of the emitted photon,
– Intra-beam scattering,
– A remnant coupling between the horizontal and vertical plane.

In most accelerators, the last point usually dominates, despite a careful set-up of the accelerator lattice that avoids coupling terms.

It is worth noting that quantum effects determine macroscopic effects such as the beam size in a synchrotron. In fact, the value of Planck's constant $\hbar$ has just the right magnitude to make practical the construction of large electron synchrotrons [3].

I.10.3.5 Some observations

I.10.3.5.1 Dependence of damping times on particle energy and type

As you can see in Equation I.10.9, the radiation power emitted by a charged particle circulating in a storage ring is inversely proportional to the fourth power of its mass, for a given energy. This fundamental relationship has profound implications for the damping times observed in electron versus proton accelerators. Electron storage rings have typically damping times on the order of tens of milliseconds. Protons, in contrast, typically emit a negligible amount of synchrotron radiation at the same energy. Consequently, the damping times of proton accelerators extend much longer, often on the order of days. In these cases, damping may typically be neglected, and the beam emittance remains constant for stored beams.

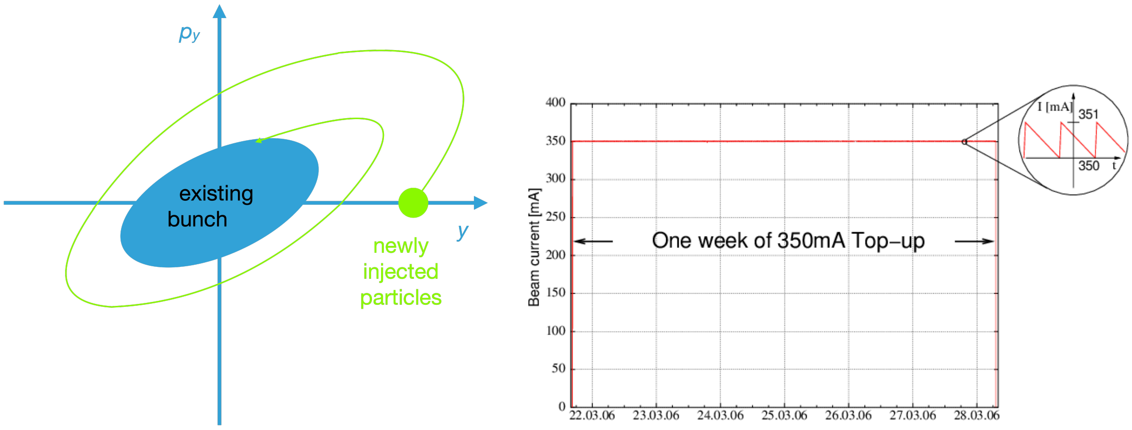

Fig. I.10.7: *Left:* Illustration of the principle of top-up injection in phase space. *Right:* Beam current in the Swiss Light Source SLS, where the beam current is held constant within less than one percent for one full week.

I.10.3.5.2 Top-up injection

Radiation damping, a distinctive feature in electron accelerators, facilitates an innovative operational mode known as *top-up injection*. In this mode, rather than filling the storage ring once and then gradually losing beam current due to scattering and other losses, the bunches stored in the accelerator continually or periodically receive additional charges. New particles are injected close to the existing bunches in phase space. Due to the presence of radiation damping, these freshly injected particles rapidly lose their excess emittance through the emission of synchrotron radiation, thereby reducing their oscillations around the ideal orbit. Consequently, they are effectively 'sucked into' the main beam, seamlessly integrating with the stored bunches.

This method contrasts with traditional filling schemes, where the beam intensity peaks right after a fill and then continuously diminishes. Top-up injection maintains a nearly constant beam current, equilibrating thermal load and thereby improving the stability of the beam over extended periods. Such consistency is particularly advantageous for user experiments, because the electron beam emits in an X-ray beam that is constant in intensity and pointing, offering more uniform conditions and reliable data. Furthermore, the ability to maintain optimal beam conditions without ramping the lattice during acceleration enhances overall time available for experiments. For this reason, virtually all modern synchrotrons make use of top-up injection (see Fig. I.10.7).

I.10.3.5.3 Robinson theorem

If we take the sum of all three partition damping numbers, noting that $j_x = 1 - \frac{I_4}{I_2}$, $j_z = 2 + \frac{I_4}{I_2}$, and using $j_y = 1$ as the vertical damping does not depend on the synchrotron radiation integrals, we can derive the *Robinson theorem*, which states that the sum of the partition numbers is 4

$$j_x + j_y + j_z = 4. \tag{I.10.43}$$

This means that the damping is not uniformly distributed along the three sub-spaces of the phase space (horizontal, vertical and longitudinal), but it is split according to specific partition numbers. These partition numbers are determined by the accelerator lattice, which gives the designers of accelerators some freedom to optimize the damping times.

I.10.4 Diffraction limited storage rings

The pursuit of higher brilliance and coherence is a driving force in the development of synchrotrons. As we have seen above, while the emission of synchrotron radiation reduces the transverse emittance of the beams in an electron synchrotron, the quantum nature of the radiation imposes a limit on how small the beam will become, and thus set a ceiling on the achievable brilliance. The source size of the X-ray beam is given by the electron beam size in the undulators. We have seen in Section I.10.3.4 that the vertical emittance is typically significantly smaller than the horizontal emittance. The vertical beam size is indeed typically so small that the X-ray beams are *diffraction-limited* in this dimension.

The term *diffraction-limited* refers to a system, typically in optics or imaging, where the resolution or image detail is primarily restricted by the fundamental diffraction of light rather than by imperfections or aberrations in the source, or in imaging components. In such a system, the performance reaches the theoretical physical limit dictated by the wave nature of the radiation. Achieving diffraction-limited performance means maximizing image sharpness and detail by minimizing all other sources of distortion or blurring to the extent that diffraction becomes the overriding factor in limiting resolution.

The horizontal emittance, conversely, is typically an order of magnitude larger. The X-ray beams are thus not diffraction-limited in this dimension. Diffraction-limited storage rings (DLSRs) overcome these constraints by minimizing the horizontal emittance to a level such that horizontal and vertical beam sizes in the undulators are similar. The diffraction limit of the X-ray beam thus becomes the defining factor for the source size, which leads to beams that are transversely fully coherent. This increased coherence translates into improved resolution and contrast in experimental techniques like X-ray imaging and scattering.

The implications of achieving diffraction-limited performance are profound. The significantly improved coherence of the X-ray beams allow scientists to use the full beam for diffraction experiments, opening doors to previously intractable scientific questions. We will now see how this is achieved, and discuss briefly the challenges for design, construction and operation.

Equation I.10.40 gives the natural horizontal emittance of the beam. A deeper inspection reveals that the main contributions to the emittance growth occur in regions where the dispersion η_x is large and the radius of curvature ρ is small, i.e. the magnetic field B is large. This makes intuitively sense. An emission of a hard X-ray photon occurs predominantly in strong magnetic fields. If this coincides with a large dispersion, the effect on the beam emittance is maximized, as the electron losing energy is now on the wrong orbit for its energy.

It is obviously impossible to build a storage ring without dispersion, or without magnetic fields. A careful design of the lattice can nevertheless minimize emittance growth in dipoles:

– **Multi-bend achromats:** unlike traditional designs that use one or two bend magnets after each straight section, a multi-bend achromat (MBA) lattice employs multiple bending magnets, inter-

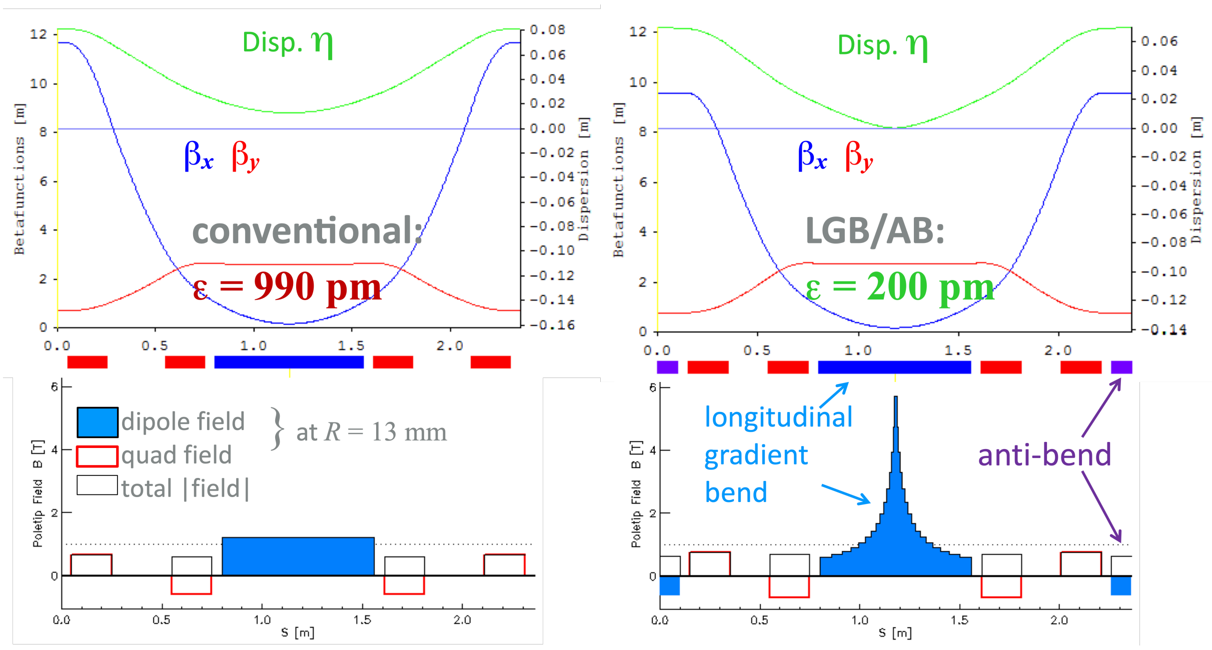

Fig. I.10.8: Comparison of conventional bend sections (left) with longitudinal gradient bends (right), as they are used in SLS-2.0. The dispersion is minimum in the center, where the quadrupoles generate a horizontal waist. In a longitudinal gradient bend, the magnetic field is maximized at this location, keeping the total field integral constant. Both sections achieve a bend angle of 6.7° for particles of an energy of 2.4 GeV. Source: Andreas Streun, PSI.

leaved with quadrupoles and sextupoles that correct for the chromaticity. The quadrupoles re-focus the beam periodically, keeping the dispersion small. By dividing the total bending angle among several magnets, the strength of each magnet can be reduced, leading to less radiation emission per bend and thus to a smaller horizontal emittance;

– **Longitudinal gradient bends:** these are dipole magnets whose magnetic field varies along their length. By providing a variable field strength along the bend, longitudinal gradient bends (LGBs) concentrate the highest magnetic field in the middle, where the dispersion reaches a minimum. This further reduces the horizontal emittance, making diffraction-limited designs possible even for small storage rings;

– **Reverse bends:** these are dipoles that have the opposite magnetic field of the regular dipoles, effectively bending the beam outwards. By carefully configuring the reverse bends, designers can disentangle horizontal focusing from dispersion matching, achieving a net reduction in beam dispersion.

Combining MBAs with LGBs and reverse bends, designers can achieve a lower horizontal emittance. For the case of SLS 2.0, the reduction in emittance is a factor 25. The combination of longitudinal gradient bends with reverse bends is shown in Fig. I.10.8.

Technical and beam dynamics considerations for diffraction-limited storage rings:

– **Magnet design:** DLSRs require a significantly more complex magnetic lattice compared to conventional storage rings. The magnetic elements in these lattices, including bending magnets, quadrupoles, and sextupoles, are not only more numerous but also often feature higher magnetic field strengths. The quadrupoles and sextupoles are therefore built with a smaller inner bore. Energy-efficient magnet designs employ permanent magnets for the basic lattice and use electromagnets only where tuning is necessary;

– **Vacuum system:** as a result of the smaller inner bore of the magnets, the vacuum chamber diameter needs to be reduced to a point where a conventional pumping system becomes difficult to implement. A key enabling technology is the use of a distributed getter pump system, where the entire vacuum chamber is coated with a non-evaporable getter (NEG);
– **Generation of hard X-rays:** the strong field in longitudinal gradient bends, peaking at 4…6 Tesla, results in very hard X-rays, up to a photon energy of 80 keV;
– **Momentum compaction factor:** when designing a magnetic lattice that employs LGBs and reverse bends, one can achieve a situation where a higher-energy particle takes a shorter path. This can then result in a negative momentum compaction factor of the ring (like in proton synchrotrons below transition energy).

The Paul Scherrer Institut is upgrading its storage ring in the year 2024, making use of the principles outlined in this section [5].

I.10.5 Interaction of X-rays with matter

In the subsequent sections, we will look at the interaction of X-rays with matter, and the use of X-rays for experiments. To understand the processes that lead to absorption, scattering, and diffraction, we will proceed in three steps, and look at the interaction of X-rays with:

– Free electrons,
– Electrons bound to an atom,
– Crystals.

The interaction of X-rays with matter is determined by the cross-section, which is itself proportional to the square of the so-called Thomson radius. The Thomson radius, in turn, is inversely proportional to the mass of the charged particle. Consequently, considering the substantial mass difference between protons and electrons, the interaction with protons can be ignored. Furthermore, neutrons, which have the same mass as protons but lack electric charge, so do not interact with electromagnetic radiation, such as X-rays. They can thus be entirely ignored.

The attenuation of X-rays in matter can be described by Beer's Law

$$I(z) = I_0 \exp(-\mu z), \tag{I.10.44}$$

where μ is the attenuation coefficient. One commonly normalizes to the density ρ, and defines the mass attenuation coefficient as μ/ρ. Values for attenuation coefficient can be found in the X-ray data booklet [6] or at `https://henke.lbl.gov/optical_constants/atten2.html`.

The relevant processes that contribute to the X-ray cross section are shown in Fig. I.10.9. Nuclear processes are only relevant for gamma rays, i.e. at photon energies far higher than what can be achieved

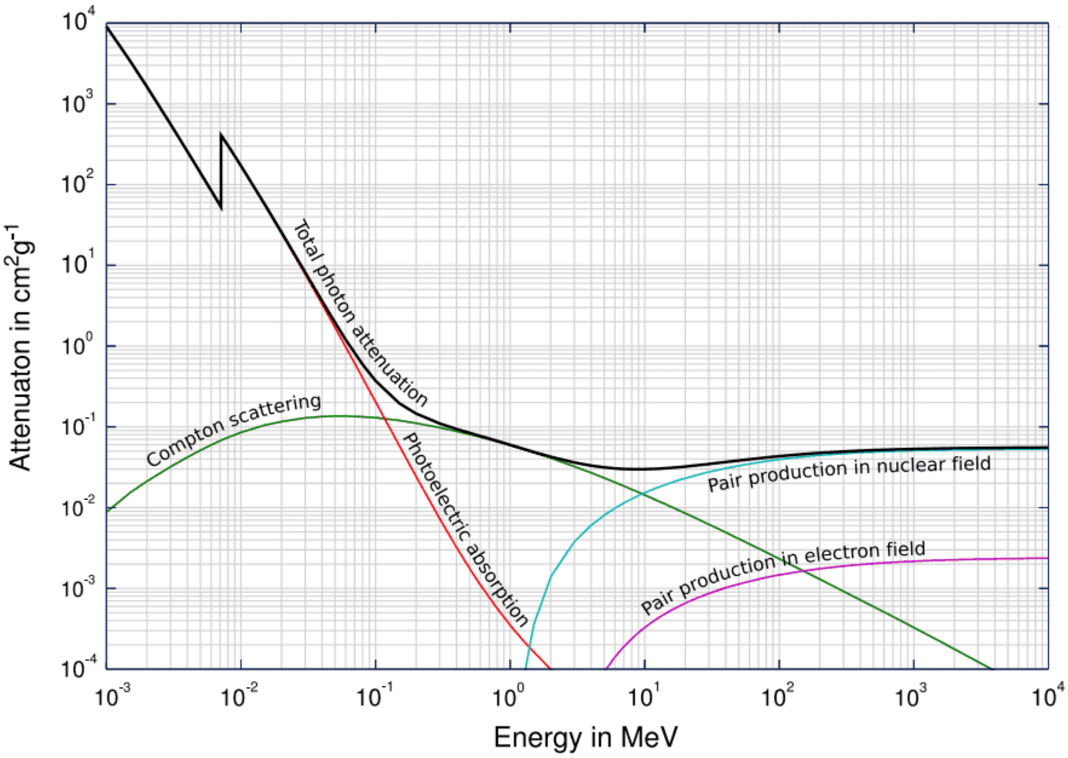

Fig. I.10.9: X-ray attenuation in matter, as a function of photon energy.

by presently available synchrotrons. Pair production can occur only for photon energies above twice the electron rest energy, 2×511 keV. The only processes relevant in synchrotrons are:

– **Photoelectric absorption:** absorption by electrons bound to atoms;
– **Thomson scattering:** elastic scattering, i.e. scattering without energy transfer between the X-ray and a free electron;
– **Compton scattering:** inelastic scattering, where energy is transferred from the X-ray photon to an electron.

I.10.5.1 Interaction of X-rays with free electrons

Thomson scattering occurs when photons with an energy that is much lower than the binding energy of electrons in atoms interact with free or loosely bound electrons. The incident photons are then scattered elastically, i.e. there is no energy transfer between the X-ray photon and the electron. The photon wavelength is inversely proportional to its energy, thus it remains constant in an elastic process. A collision, however, implies in general a change in direction, thus the momentum $\vec{k}$ of the photon will change its direction.

We can describe Thomson scattering by classical electromagnetism, considering a free electron that encounters an electromagnetic wave. The electron will start oscillating and radiate in all directions except the direction of the oscillation, with an intensity given by $I = I_0 \cos^2 \vartheta$. This re-radiated light has the same frequency as the incident light because the electron's oscillation frequency is driven by the frequency of the electromagnetic wave, and there's no energy loss in the system.

The scattering amplitude I_0 can be calculated from classic electromagnetism. For non-relativistic electrons, it is sufficient to consider the electric component of the incoming wave. The Thomson scattering cross section is equal to

$$\sigma_T = \frac{8\pi}{3}\left(\frac{e^2}{4\pi\varepsilon_0 m_e c^2}\right)^2 = 0.6 \cdot 10^{-28}\,\mathrm{m} = 0.6\,\mathrm{barn}, \tag{I.10.45}$$

independent of the wavelength of the incoming photon.

This is in contrast to *Compton scattering*, where we consider photons with an energy above a few 10 keV. In this case, we have to consider quantum mechanical effects, and the photon transfers energy and momentum to the electron. The wavelength change of the scattered photon can be determined from the conservation of energy and momentum

$$\Delta\lambda = \frac{h}{m_e c}(1 - \cos\vartheta), \tag{I.10.46}$$

where ϑ is the angle at which the photon is scattered.

I.10.5.2 Scattering of X-rays on atoms

In the case of photon energies less than a few keV, the wavelength is longer than the size of the atom. The scattering is then coherent, i.e., the phases of the scattered waves from different parts of the electron cloud add up constructively. The electric field amplitude of the scattered wave is then proportional to the total number of electrons in the atom Z, and the scattered intensity is proportional to Z^2. The total cross section is then

$$\sigma = Z^2 \sigma_T. \tag{I.10.47}$$

The Z^2 dependence makes the scattering cross section for heavier atoms much larger compared to lighter ones, significantly influencing how X-rays are used in science and medicine.

When we increase the photon energy, the wavelength becomes smaller than the size of the electron cloud of an atom, and decoherence between the scattered waves reduces the scattering cross section. As an approximation, the cross-section drops off as $1/E_\gamma^2$. The precise drop-off can be described by the atomic form factor f^0, which depends on both the scattering angle and the photon wavelength. It can be parametrized as

$$f^0(\sin(\vartheta)/\lambda) = \sum_{i=1}^{4} a_i \exp\left[-b_i\left(\frac{\sin\vartheta}{\lambda}\right)^2\right] + c,$$

where $a_1, \ldots, a_4$, $b_1, \ldots, b_4$ and c are tabulated in the International Tables of Crystallography [7].

Different additional processes can occur when an X-ray photon with a higher energy interacts with an electron bound to an atom:

- **Refraction and reflection:** similarly to the description of visible electromagnetic radiation, the elastic interaction between X-rays and matter can be described by refraction and reflection. The index of refraction of most materials for X-rays is very close to, but slightly smaller than, one. This has some notable consequences: concave lenses focus an X-ray beam, but the focal length is very large; also, at very low angles of incidence (grazing angles), X-rays can be effectively reflected by total external reflection. This phenomenon is central to the design of X-ray mirrors;

- **Elastic scattering:** in contrast to Thomson scattering, which occurs for free electrons, *Rayleigh scattering* describes the scattering on bound electrons, incorporating the quantum mechanical nature of the atoms;
- **Inelastic scattering:** while we looked at free electrons previously, Compton scattering can still occur with weakly bound electrons in heavier atoms where the binding energy is much lower than the energy of the incident X-ray photon;
- **Photoelectric effect:** when the energy of the incoming photon is greater than the binding energy of the electron in the atom, it can be completely absorbed, ejecting the bound electron (now referred to as a photoelectron) from the atom. The energy of the photoelectron is equal to the energy of the incident X-ray photon minus the binding energy of the electron in its original orbital;
- **Absorption edges:** the requirement that X-rays have a minimum energy to ionize an electron in a given orbital leads to the formation of absorption edges. These edges are specific to each element, and are widely used to characterize samples;
- **Fluorescence:** when an inner-shell electron is ejected (as in the photoelectric effect), an electron from a higher energy level falls into the lower energy vacancy, emitting an X-ray photon with a characteristic energy specific to the atom;
- **Auger electrons:** similarly to fluorescence, this effect starts with the ionization or excitation of an inner-shell electron due to the interaction with the X-ray photon. This leaves a vacancy in the inner shell, which is then filled with an outer-shell electron. However, instead of releasing the excess energy as a photon, the energy is transferred non-radiatively to another outer-shell electron. This transfer of energy gives the second electron enough energy to be ejected from the atom, resulting in the emission of what is known as an Auger electron.

These processes are summarized in Fig. I.10.10.

Inelastic processes always lead to an energy deposition in the material, often leading to radiation damage, which limits the exposure time in many X-ray experiments.

I.10.5.3 Crystal diffraction

Imagine many atoms, arranged in a regular lattice, illuminated by a coherent X-ray source. The elastic scattering on the electron clouds of these atoms will add constructively if all individual waves are in phase. This situation is shown in Fig. I.10.11. Considering a distance d between the crystal planes, and referring to the notation in this figure, we get constructive interference when

$$(AB + BC) - (AC') = n\lambda$$

for any natural number n.

$$AB = BC = \frac{d}{\sin\vartheta}$$

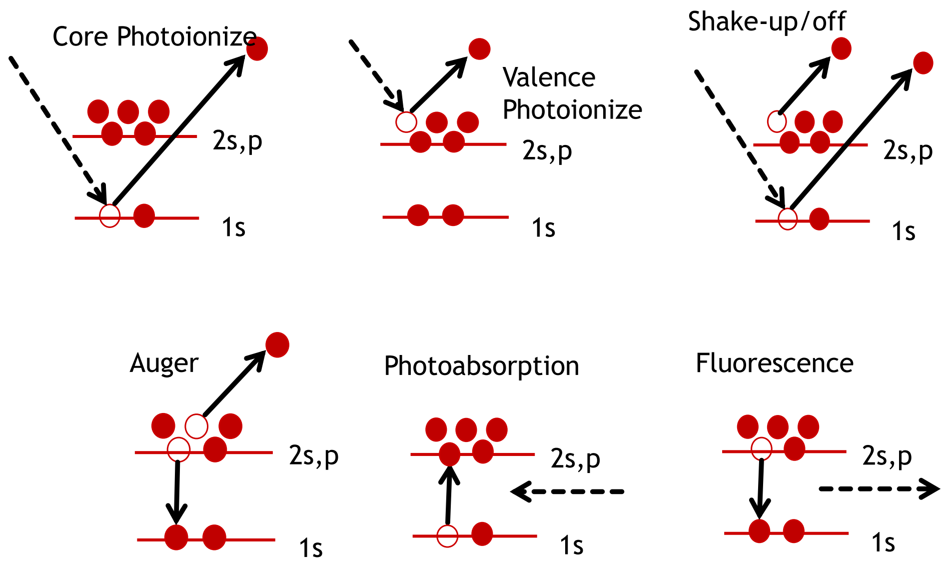

Fig. I.10.10: Processes that can occur when an X-ray photon interacts with the electrons in an atom. Source: Phil Bucksbaum, Stanford.

and

$$AC = \frac{2d}{\tan\vartheta},$$

from which follows

$$AC' = AC\cos\vartheta = \frac{2d}{\tan\vartheta}\cos\vartheta = \frac{2d}{\sin\vartheta}\cos^2\vartheta,$$

and we conclude

$$\begin{aligned} n\lambda &= \frac{2d}{\sin\vartheta} - \frac{2d}{\tan\vartheta}\cos\vartheta = \frac{2d}{\sin\vartheta}(1-\cos^2\vartheta) = \frac{2d}{\sin\vartheta}\sin^2\vartheta \\ &= 2d\sin\vartheta, \end{aligned} \tag{I.10.48}$$

which is Bragg's law. Note that contrary to the diffraction on a two-dimensional surface, which is often considered fir visible light, X-rays diffract on a three-dimensional crystal lattice. In this case, not only the exit angle matters, but also the incoming angle must fulfill the resonance condition!

X-ray diffraction is one of the key techniques to resolve molecular structure in samples that can be crystallized. In the following section, we will look at different applications of synchrotron radiation in science, medicine and industry.

I.10.6 Applications of synchrotron radiation

Synchrotron radiation is used in a wide range of scientific and industrial applications, and over 60 synchrotron radiation sources are operating around the world. New facilities are under construction, reflecting the growing demand in research and industrial applications.

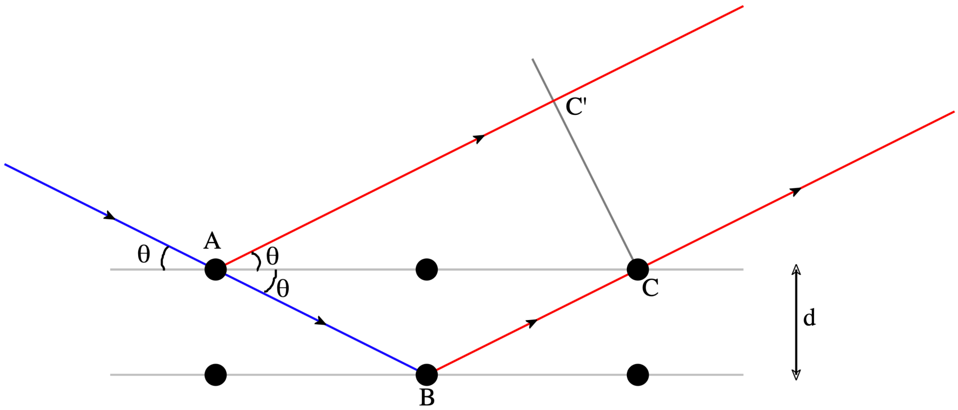

Fig. I.10.11: Scattering of X-rays off atoms in a crystal results in constructive interference at specific entry and exit angles. Source: M. Hadjiantonis, Wikimedia Commons.

Fig. I.10.12: *Left:* Photo 51, the diffraction pattern of a DNA crystal, recorded by Rosalind Franklin and Raymond Gosling. *Right:* James Watson and Francis Crick, in front of a model of DNA. Source: Wikimedia Commons.

I.10.6.1 Diffraction

Coherent diffraction on crystals has been used before the emergence of synchrotrons, at the time enabled by X-ray tubes. The renowned Photo 51, recorded by Rosalind Franklin and her student Raymond Gosling, found its way (through dubious ways) into the hands of James Watson and Francis Crick, who used it to decipher the double helix structure of DNA (see Fig. I.10.12).

Why do scientists use diffraction in place of imaging to determine the structure of molecules? Would it not be easier to simply magnify the X-ray image onto a detector, as we do in transmission electron microscopes?

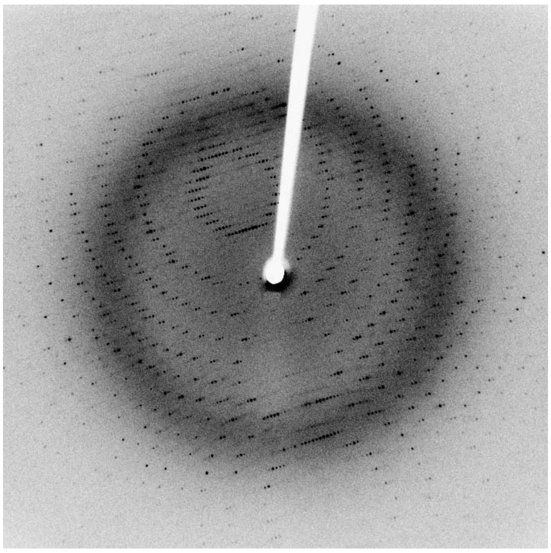

Fig. I.10.13: Diffraction pattern of crystallized 3C-like protease from the SARS coronavirus. Source: Jeff Dahl, Wikimedia Commons.

The size of an atom is on the order of 1 $\text{Å} = 10^{-10}$ m, while the pixels of an X-ray detector are around 100 μm in size. A magnification of 10^6 would thus be required, and it turns out that no X-ray lens can provide this[9]. Unlike lenses for visible light, where glasses of different index of refraction and different dispersion can be combined to compensate lens errors, this is not possible for X-rays. Scientist use thus diffractive imaging, where a computer is used to reconstruct the distribution of atoms in the molecule from the diffraction pattern.

When a crystal is placed in a coherent X-ray beam, constructive interference occurs if the Bragg condition (Equation I.10.48) for the incoming and outgoing rays is fulfilled for any given crystal plane. The resulting diffraction pattern appears as a series of spots or fringes, commonly captured on a detector. As an example, the diffraction pattern of a complex biomolecule is shown in Fig. I.10.13. The crystal is then rotated to change the incoming angle, to allow for diffraction from other crystal planes to be recorded. Note that the detector records the number of photons, i.e., the intensity of the diffracted wave, but all phase information is lost.

One thus receives a series of two-dimensional diffraction patterns. The intensities of the diffracted spots relate to the absolute square of the Fourier transform of the electron density, and their positions correspond to the inverse of the spacing between planes of atoms in the crystal, as described by Bragg's law.

However, directly computing the electron density from the diffraction pattern is not straightforward due to the phase problem: the detector records only the intensity of the diffracted waves, losing information about their phases. In essence, we only measure the amplitude of the Fourier transform, not its phase, yet both are necessary for accurate reconstruction. Various methods, such as using a known similar structure as a model (molecular replacement) or adding heavy atoms to the crystal (multiple

[9]Photographic film has a resolution of about 1 μm, thus a magnification of 10^4 would be required in this case, but even that is not achievable.

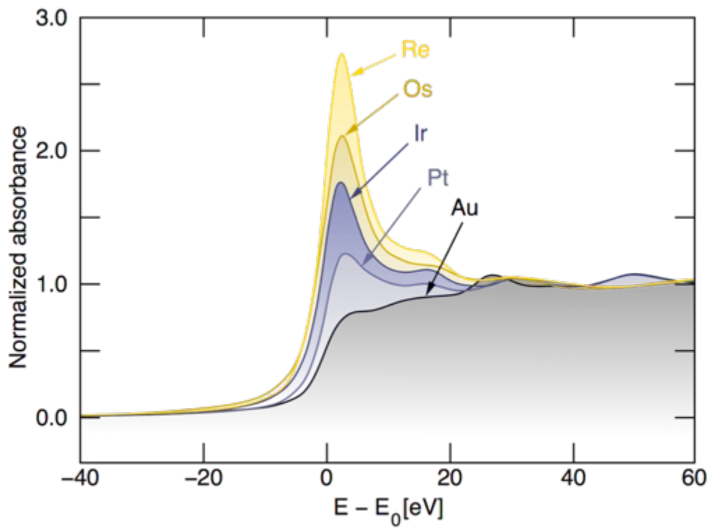

Fig. I.10.14: The detailed shape of an X-ray absorption edge can be used to infer the chemical composition of a sample. This is used in X-ray absorption near edge structure (XANES). Source: G. Meitzner et al. J. Phys. Chem. 96 4960 (1992).

isomorphous replacement), help in estimating these phases.

Once the phases are estimated and combined with the intensities, the inverse Fourier transform is used to compute the electron density. The peaks in this electron density map correspond to the locations of the atoms in the crystal. By interpreting this map, scientists can determine the precise arrangement of atoms and thus the molecular structure of the sample. Machine learning (ML) is emerging as a powerful tool in various stages of structure determination from X-ray crystallography data.

I.10.6.2 Spectroscopy

Spectroscopic methods are used for investigating the electronic structure, chemical composition, and dynamic properties of matter. X-ray absorption spectroscopy (XAS) techniques, including X-ray absorption near edge structure (XANES), Extended X-ray Absorption Fine Structure (EXAFS) and Near Edge X-ray Absorption Fine Structure (NEXAFS), use the sudden change in absorption near edges (Section I.10.5.2) to probe the local atomic structure and electronic states of specific elements within a material (see Fig. I.10.14). Absorption edges, related to the ionization potential of inner-shell electrons in an atom, have a very small dependence on the chemical configuration of the atom in a molecule, as this shifts the energy levels slightly.

X-ray fluorescence (XRF) is based on the principle that when a material is irradiated with X-rays, electrons from the inner shells of the atoms in the material can be ejected, leading to the emission of fluorescence X-rays as electrons from higher energy levels fill these vacancies. The energy of the emitted fluorescence X-rays is characteristic of each element, thus enabling qualitative and quantitative analysis of the elemental composition of the sample (see Fig. I.10.15). Similarly, X-ray photoelectron spectroscopy (XPS) measures the kinetic energy and the number of electrons that are emitted from the sample upon X-ray irradiation. Since the mean free path of free electrons in solids is only a few

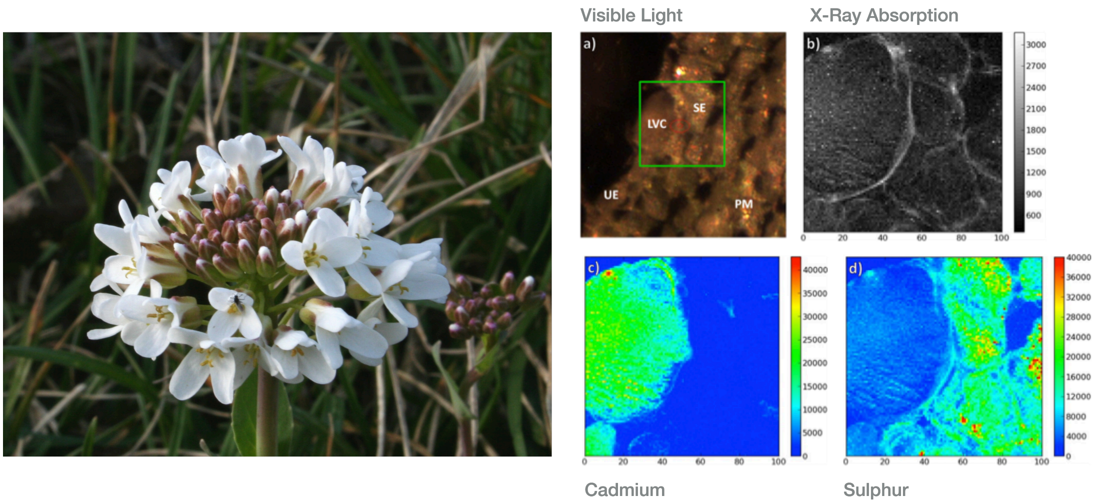

Fig. I.10.15: The flower Thlaspi Praecox, native to Pakistan, is known to absorb lead, cadmium and tin from the soil. The exact location of the cadmium-absorbing cells is visualized with spatially resolved X-ray fluorescence spectroscopy. Sources: Wikimedia Commons (left); Koren et al., Plant and Soil 370 1-2 125 (2013) (right).

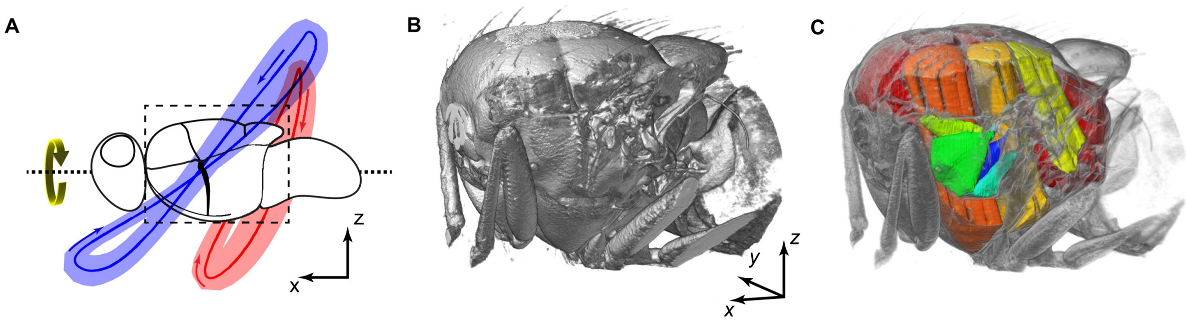

Fig. I.10.16: Arrangement of the muscles in the thorax of a fly. A movie detailing these muscles can be seen at `https://youtu.be/P61BkK3J9wg?si=-pXEG7nFPiG587WO`. Source: Walker, Schwyn et al., PLOS Biology 12(3): e1001823 (2014).

molecular layers, this technique enables the study of surface chemistry. Angular-resolved photoelectron spectroscopy (ARPES) allows reconstructing the momentum of the electrons in the solid, which is used to reconstruct the electronic band structure of the material.

I.10.6.3 Tomographic imaging and ptychography

Tomography is a powerful imaging technique that reconstructs a three-dimensional object from its two-dimensional projections. It is used widely in medicine, where it allows a detailed view of our skeleton. Synchrotron radiation sources, with their brilliant and monochromatic beams, allow reducing the exposure time to less than a millisecond while achieving micrometer resolution. This makes the technique useful for research in fields ranging from materials science to biology (see Fig. I.10.16).

The process involves rotating the sample through a range of angles relative to the X-ray beam, while collecting a series of two-dimensional absorption images. The three-dimensional distribution is reconstructed from the two-dimensional images.

The monochromatic and coherent X-ray beams from a synchrotron allow recording phase contrast images, which can capture finer details of biological samples than the usual absorption contrast images.

In *ptychography*, a coherent X-ray beam is scanned across the sample in overlapping patterns, and the diffraction pattern from each area is recorded. These overlapping diffractions provide redundant information. The reconstruction algorithms used in ptychography are able to retrieve both the amplitude and phase information from the scattered wavefronts, leading to highly detailed images with nanometer resolution. Ptychography is particularly advantageous for studying materials with fine structural details and can be applied to a wide range of materials, including biological specimens, nanomaterials, and integrated electronic circuits (see e.g. https://youtu.be/GvyTiK9CNO0).

Synchrotron sources, with their intense and coherent X-ray beams, play a crucial role in both tomographic imaging and ptychography. They provide the necessary beam brightness and coherence, enabling the capture of high-resolution data and facilitating the reconstruction processes.

I.10.7 Collection of exercises

The subsequent section collects an assortment of problems discussed in tutorials, and used in the written exams at JUAS. Note that the exams were open-book exams, where personal notes and course material, as well as reference booklets were allowed.

You can find solutions to these exercises at https://ischebeck.net/juas/book/solutions.pdf

I.10.7.1 Energy and momentum

An electron is accelerated by a DC voltage of 1 MV. What is its total energy?

a) $E = 1\,\mathrm{MeV}$

b) $E = 1\,\mathrm{MeV} + 511\,\mathrm{keV} = 1.511\,\mathrm{MeV}$

c) $E = \sqrt{1^2 + 0.511^2}\mathrm{MeV} = 1.123\,\mathrm{MeV}$

d) This depends on the particle trajectory.

What is the momentum of the particle?

I.10.7.2 Brilliance

Estimate the brilliance $\mathcal{B}$ of the sun on its surface, for photons in the visible spectrum.
What is the brilliance of the sun on the surface of the Earth? For simplicity, ignore the influence of the Earth's atmosphere.

Sun		
Radiated power	$3.828 \cdot 10^{26}$	W
Surface area	$6.09 \cdot 10^{12}$	km^2
Distance to Earth	$1.496 \cdot 10^{8}$	km
Angular size, seen from Earth	$31.6 \ldots 32.7$	minutes of arc
Age	$4.6 \cdot 10^{9}$	years

I.10.7.3 Synchrotron radiation

Synchrotron radiation... (check all that apply: more than one answer may be correct)

a) ... is used by scientists in numerous disciplines, including semiconductor physics, material science and molecular biology

b) ... can be calculated from Maxwell's equations, without the need of material constants

c) ... is emitted at much longer wavelengths, as compared to cyclotron radiation

d) ... is emitted uniformly in all directions, when seen in the reference frame of the particle

e) ... is emitted in forward direction in the laboratory frame, and uniformly in all directions, when seen in the reference frame of the electron bunches

I.10.7.4 Crab Nebula

On July 5, 1054, astronomers observed a new star, which remained visible for about two years, and it was brighter than all stars in the sky (with the exception of the Sun). Indeed, it was a supernova, and the remnants of this explosion, the Crab Nebula, are still visible today. It was discovered in the 1950's that a significant portion of the light emitted by the Crab Nebula originates from synchrotron radiation (Fig. I.10.17).

Radiation is emitted by electrons with a wide energy spectrum. As an example, calculate the critical energy of the photons emitted by 300 GeV electrons in a uniform magnetic field of 30 nT!

How can astrophysicists distinguish light that originates from synchrotron radiation from black body radiation?

I.10.7.5 Large Hadron Collider

A proton circulates in LHC. Assume a circumference of 26.7 km, a particle energy of 6.5 TeV, and a magnetic field of 7.7 T. Calculate:

- The Lorentz factor γ,
- The radius of curvature that the protons make in the dipoles,
- The critical energy of the synchrotron radiation,
- The energy emitted through synchrotron radiation in the dipoles by one proton in one turn,
- Which fraction of the circumference is occupied by dipole magnets?

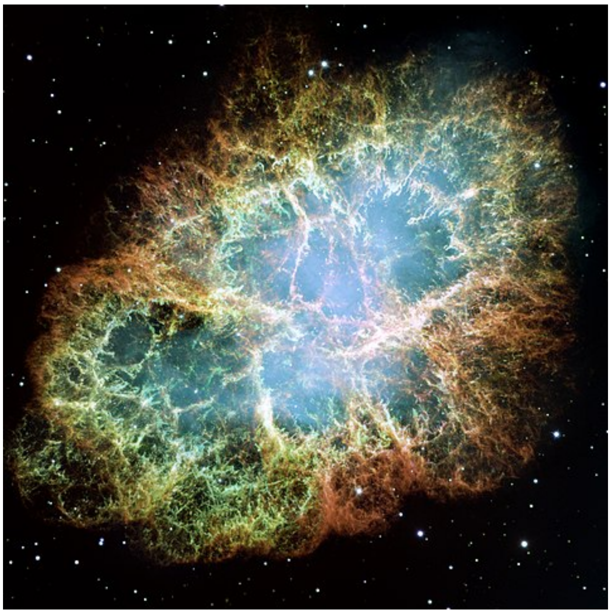

Fig. I.10.17: The Crab Nebula. Source: Wikimedia Commons.

I.10.7.6 Future Circular Collider: FCC-ee

As a first step towards a future circular collider, physicists are considering an electron accelerator with 100 km circumference (FCC-ee). The production of Higgs bosons (through the ZH channel) is maximized when running this ring on resonance at a particle energy of 120 GeV. For an electron circulating in this ring, calculate:

- The Lorentz factor γ,
- The magnetic field to bend the beam (assume for simplicity that the ring consists of a uniform dipole field),
- The critical energy of the synchrotron radiation,
- The energy emitted by each electron through synchrotron radiation in one turn.

I.10.7.7 Future Circular Collider: FCC-hh

Particle physicists are evaluating the potential of building a future circular collider, which aims at colliding two proton beams with 500 mA current each and 100 TeV particle energy (FCC-hh). The protons would be circulating in a storage ring with 100 km circumference, guided by superconducting magnets. The dipoles aim at a field of 16 T. Calculate:

- The Lorentz factor γ,
- The critical energy of the synchrotron radiation,
- The total power emitted by both beams through synchrotron radiation.

I.10.7.8 Simple storage ring

Let's build a very simple synchrotron! Consider a storage ring that is located at the (magnetic) North Pole of the Earth. Assume that the Earth's magnetic field of 50 μT is used to confine electrons to a circular orbit, and ignore the need for focusing magnets. As a particle source, we will use the electron gun of an old TV, which accelerates the particles with a DC voltage of 25 kV (we will ignore the requirement of an injection system).

Why is the North Pole the preferred site for this experiment? What will be the circumference of this storage ring? Calculate the radiated power per electron!

How would the situation change if we used protons with the same momentum?

I.10.7.9 Permanent magnet undulators

Which options exist to tune the photon energy of coherent radiation emitted by a permanent magnet undulator (give two options)?
How is the critical photon energy from each dipole in the undulator affected by these two tuning methods? What are the consequences?

I.10.7.10 Superconducting undulators

Which options exist to tune the photon energy of coherent radiation emitted by a superconducting undulator (give two options)?

I.10.7.11 Undulator

An undulator has a length of 5.1 m and a period $\lambda_u = 15$ mm. The pole tip field is $B_t = 1.2$ T. For a gap of $g = 10$ mm, calculate:

- The peak field on axis B_0,
- The undulator parameter K.

The undulator is installed in a storage ring with an electron beam energy of $E = 3$ GeV. Assume electron a beam current of 500 mA, beam emittances of $\varepsilon_x = 1$ nm and $\varepsilon_y = 1$ pm, alpha functions $\alpha_x = \alpha_y = 0$, beta functions of $\beta_x = 3.5$ m and $\beta_y = 2$ m, and calculate:

- The wavelength of radiation emitted on axis,
- The relative bandwidth,
- The photon flux (*hint:* if your calculator cannot evaluate Bessel functions, you may read the value of $Q_n(K)$ from the plot in the lecture),
- The electron beam size and divergence,
- The effective source size and divergence,
- The brilliance of the radiation at the fundamental wavelength.

I.10.7.12 Undulators

The energy of a synchrotron is increased by 10%, keeping the beam optics (i.e. the lattice) and the current constant. The synchrotron has an undulator. Assume that the synchrotron radiation integral I_2 along the undulator is negligible in comparison to the total integral around the ring, and that the dispersion is zero in the undulator: $D_x = D_{x'} = 0$. We will initially assume that the undulator period, the pole tip field, and the gap are unchanged.

- By how much is the horizontal beam emittance changed?
- By how much is the photon energy of the fundamental radiation from the undulator changed?
- By how much is the brilliance of the undulator radiation changed? Assume that the effective source size is dominated by the radiation in the vertical plane, and by the electron beam phase space in the horizontal plane.

How is the situation different when one decreases the gap to keep the photon energy constant? Describe qualitatively the effects on the undulator parameter K and the brilliance $\mathcal{B}$!

I.10.7.13 Muons

Muons are considered as an alternative to electrons for a future circular lepton collider. Argue

- Why they might be preferable to electrons?
- What could be possible disadvantages?

I.10.7.14 Electrons vs. muons

Consider an electron storage ring at an energy of 800 MeV, a circulating current of 1 A, and a bending radius of $\rho = 1.784$ m. Calculate the energy loss of each electron per turn, and the total synchrotron radiation power from all bending magnets.
What would the radiation power be if the particles were 800 MeV muons?

I.10.7.15 Swiss Light Source 2.0

Calculate how much energy is stored in the electron beam in the SLS-2.0 storage ring, with a circumference of 290.4 m and an average current of 400 mA. The particle energy is 2.4 GeV. Assume the RF trips off. Knowing that the momentum acceptance is $\pm 5\%$, compute how long the beams survives in the ring before hitting the wall.

I.10.7.16 Critical energy

For the electron beam of the previous exercise, calculate the critical photon energy ε_c that is emitted by the superbends with $B = 6$ T, and draw a sketch of the radiation spectrum. What is the useful photon energy range for experiments, assuming that the spectral intensity should be within 1% of the maximum value?

I.10.7.17 Critical frequency

What do we understand by *critical frequency?*

a) The frequency ω_c at which a storage ring becomes unstable

b) The frequency of the photons coming from an undulator

c) The frequency ω_c at which the integrated spectral density of photons with $\omega < \omega_c$ is 50% of the total energy radiated

d) The revolution frequency of the electrons in a synchrotron

e) The frequency ω_c where the highest spectral density of photos is emitted

f) The frequency ω_c at which critical components fail

I.10.7.18 Undulator radiation

Assume an undulator of 18 mm period and 5.4 m length. The pole tip field is $B_t = 1.5$ T, and the gap can be varied between 10 and 20 mm.
This undulator is placed in a storage ring, with an electron beam energy of $E = 4$ GeV, and a beam current of 400 mA. The beam is focused to a waist of $\sigma_x = \sigma_y = 20$ µm inside the undulator.

- What range can be reached with the fundamental photon energy?
- What brilliance can be reached at the fundamental photon energy?
- Is there a significant flux higher harmonics?

I.10.7.19 Undulator radiation

Assume an undulator of 15 mm period and 5 m length. The pole tip field is $B_t = 1.5$ T, and the gap can be varied between 8 and 16 mm.
This undulator is placed in a storage ring, with an electron beam energy of $E = 3.2$ GeV, and a beam current of 500 mA. The beam is focused to a waist of $\sigma_x = \sigma_y = 20$ µm inside the undulator.

- What range can be reached with the fundamental photon energy?
- What brilliance can be reached at the fundamental photon energy?
- Is there a significant flux higher harmonics?

I.10.7.20 Emittance and energy spread

The equilibrium emittance of an electron bunch in a storage ring occurs when factors increasing ε are compensated by those reducing ε.

- Which effect increases the horizontal emittance ε_x?
- Which effect decreases the horizontal emittance ε_x?
- Which effect increases the vertical emittance ε_y?
- Which effect decreases the vertical emittance ε_y?

I.10.7.21 Swiss Light Source

The Swiss Light Source (SLS) is a storage ring optimized for synchrotron radiation generation, located at PSI in Switzerland. An upgraded lattice has been calculated in view of an upgrade[10].

Design values for this lattice are given below (the synchrotron radiation integrals have been numerically integrated around the design lattice, including undulators and superbends for radiation generation):

SLS Upgrade Lattice		
Circumference	290.4	m
Electron energy	2.4	GeV
Horizontal damping partition j_x	1.71	
Vertical damping partition j_y	1	
Longitudinal damping partition j_z	1.29	
Second synchrotron radiation integral I_2	1.186	m^{-1}
Fourth synchrotron radiation integral I_4	-0.842	m^{-1}

Calculate the damping times in the horizontal (x) and vertical (y) phase spaces, as well as in the energy/time phase space!

I.10.7.22 Large Hadron Collider

The Large Hadron Collider at CERN collides protons in a storage ring with 27 km circumference. Assuming that synchrotron radiation is only emitted in the dipoles in the arcs, which have a bending radius of 2900 m, calculate the following parameters for protons with an energy of 7 TeV:

- The energy loss per turn, per particle,
- The critical photon energy of synchrotron radiation,
- The vertical damping time.

How does these numbers compare to LEP (assuming the same circumference and dipole bending radius) at an electron energy of 100 GeV?

I.10.7.23 Preparation for an upgrade

Petra-III is a 2.3 km circumference light source at 6 GeV and 1 nm horizontal emittance, located at DESY in Hamburg. An upgrade based on multi-bend achromats will decrease the emittance to 10 pm. Before the upgrade, the DESY team wants to test instrumentation for the new ring at low emittance.

Suggest a way to lower the emittance at the existing machine in order to test the instrumentation. What are some issues with your suggestion?

I.10.7.24 Upgrade

The SLS 2.0 Upgrade, amongst other things, considers an increase of the electron energy from 2.4 to 2.7 GeV.

[10] A. Streun (ed.): SLS-2 Conceptual Design Report. PSI-Bericht 17-03, December 21, 2017.

– What can be the rationale for this change? Assume that the lattice is the same for both energies.
– Are there detrimental aspects to an energy increase?

I.10.7.25 Neutron star

A proton with energy $E_p = 10$ TeV moves through the magnetic field of a neutron star with strength $B = 10^8$ T.

– Calculate the diameter of the proton trajectory and the revolution frequency.
– How large is the power emitted by synchrotron radiation?
– How much energy does the proton lose per revolution?

I.10.7.26 Cosmic electron

A cosmic electron with an energy of 1 GeV enters an interstellar region with a magnetic field of 1 nT. Calculate:

– The radius of curvature,
– The critical energy of the emitted synchrotron radiation,
– The energy emitted in one turn.

How would you measure this radiation?

I.10.7.27 Superconducting undulators

What is the advantage of using undulators made with superconducting coils, in comparison to permanent-magnet arrays? What are drawbacks?

I.10.7.28 In-vacuum undulators

What are the advantages of using in-vacuum undulators? What are possible difficulties?

I.10.7.29 Instrumentation

How would you measure the vertical emittance in a storage ring?

I.10.7.30 Top-up operation

What are the advantages of top-up operation? What difficulties have to be overcome to establish top-up in a storage ring? (give one advantage and one difficulty for 1P.; give one more advantage and one more difficulty for 1P.$\star$.)

I.10.7.31 Fundamental limits

The SLS 2.0, a diffraction limited storage ring, aims for an electron energy of 2.4 GeV and an emittance of 126 pm. How far is this away from the de Broglie emittance, i.e. the minimum emittance given by the uncertainty principle?

I.10.7.32 Applications

Why are synchrotrons important for science?

I.10.7.33 Applications

What applications for industry are there to synchrotrons?

I.10.7.34 Orbit correction

Which devices are used to measure and correct the orbit inside a synchrotron?

I.10.7.35 Instrumentation

How would you measure the bunch length in a synchrotron?

I.10.7.36 Instrumentation

How would you measure the stability of the orbit in a storage ring?

I.10.7.37 Detection

What possibilities exist to detect X-Rays? How has the development of X-ray detectors influenced experiments at synchrotron sources?

I.10.7.38 Monochromators

What dispersive element is used to monochromatize X-Rays? What differences exist to monochromators for visible light?

I.10.7.39 Refractive index

The passage of electromagnetic radiation can be described classically by an index of refraction. What are the properties of the index of refraction of most materials at X-ray wavelengths?

I.10.7.40 DLSRs

How do longitudinal gradient bends contribute towards the goal of achieving a lower horizontal emittance in a diffraction limited storage ring?

I.10.7.41 Diffraction limited storage rings

Which of the following methods are employed to reduce the horizontal emittance in the DLSR SLS 2.0?

a) Minimize the dispersion in areas of large dipole fields

b) Maximize coupling between horizontal and vertical plane

c) Increase the beam pipe diameter to reduce wake fields

d) Alternate between insertion devices with horizontal and vertical polarization

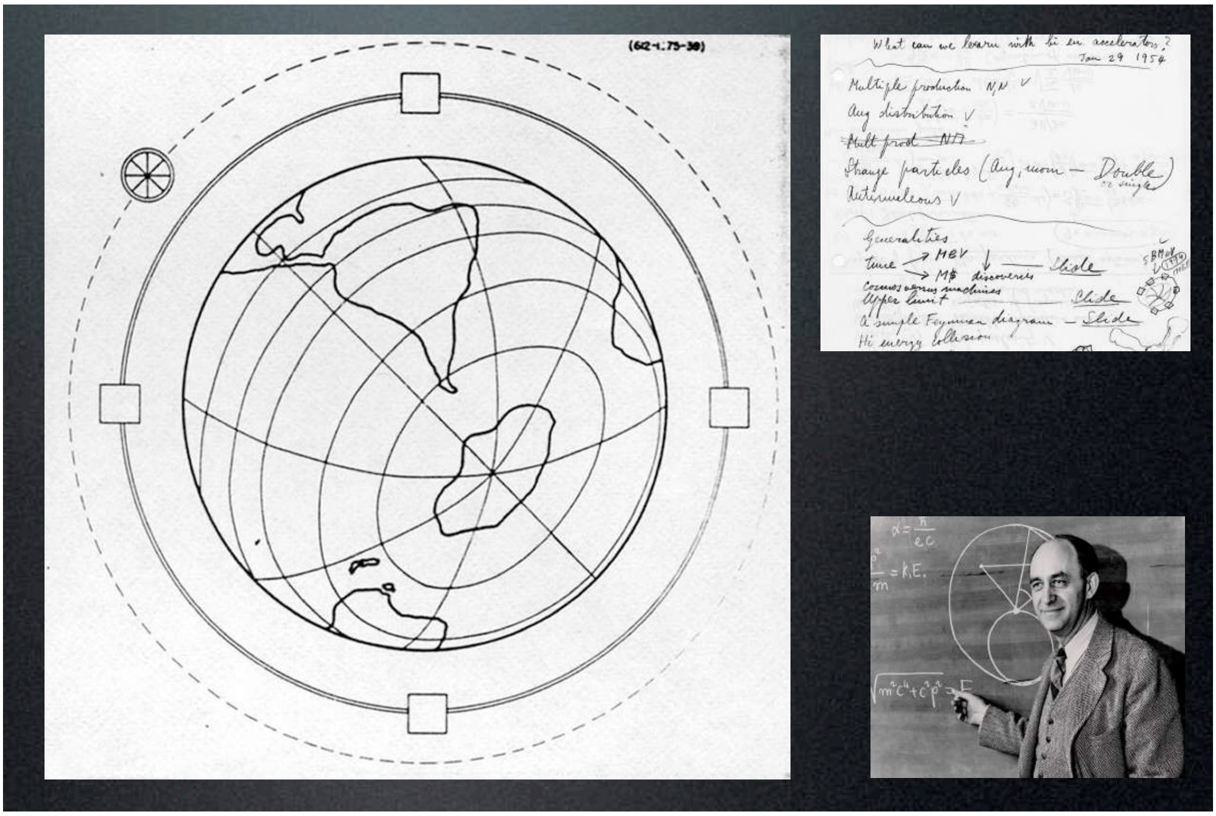

Fig. I.10.18: Enrico Fermi proposing the Globatron.

I.10.7.42 Globatron

Enrico Fermi proposed the Globatron, a storage ring for protons suspended in space around the earth. This would have 5 PeV proton beams in a ring with 8 000 km radius (Fig. I.10.18). Calculate:

- The required magnetic field in the dipoles,
- The losses through synchrotron radiation per particle per turn.

How would the situation change for electrons of the same energy? Calculate the required magnetic field in the dipoles, and the synchrotron losses!

I.10.7.43 A particle accelerator on the Moon

Imagine a particle accelerator around the circumference of a great circle of the Moon (Fig. I.10.19) [8]. Assuming a circumference of 11 000 km, and a dipole field of 20 T, what center-of-mass energy could be achieved

- For electrons?
- For protons?

For simplicity, assume the same dipole filling factor as in LHC, i.e. 67% of the circumference is occupied by dipole magnets. What is the fundamental problem with the electron accelerator? *(hint: calculate the*

Fig. I.10.19: The Mooon. Source: Wikimedia Commons.

synchrotron radiation power loss per turn, and compare to the space available for acceleration. Which accelerating gradient would be required?)

Calculate the horizontal damping time for proton beams circulating in this ring. What are the implications for the operation?

I.10.7.44 Diffraction

Why is diffraction often used in place of imaging when using X-rays?
What is the *phase problem* in X-ray diffraction?

I.10.7.45 Crystals

Which of the following are crystalline (more than one answer is may be correct)?

a) The glass on the screen of my mobile phone

b) The sapphire glass on an expensive watch

c) Asbestos

d) Icing sugar

e) Sapphire

f) Fused silica

g) Snowflakes

h) Paracetamol (Acetaminophen) powder in capsules

i) The DNA in my body

k) A diamond

l) Viruses

Why are crystals important for diffractive imaging?

How is the X-ray diffraction from quartz different from that of fused silica?

I.10.7.46 Absorption and diffraction

A scientist wants to record a diffraction pattern of a silicon crystal at a photon energy of 8 keV. What is the optimum thickness of the crystal, that maximizes the intensity of the diffracted spot?
Hint: you can find the mass absorption coefficient of silicon on page 1-41 (page 49 in the PDF) of the X-Ray Data Booklet, and the density on page 5-5 (page 153).

I.10.7.47 Detectors

Name two or more advantages of semiconductor detectors, as compared to Röntgen's photographic plates!

I.10.7.48 X-ray absorption

What is the dominant process for X-Ray absorption of

- 10 keV photons
- 1 MeV photons
- 100 MeV photons

in matter?

I.10.7.49 Diffraction

A scientist wants to record a diffraction pattern of crystalline tungsten at a photon energy of 20 keV. What is the optimum thickness of the crystal, that maximizes the intensity of the diffracted spot? Derive the formula for the intensity I of the diffracted spot as a function of thickness z, and solve for $dI/dz = 0$. Material constants can be found in the X-Ray Data Booklet.

I.10.7.50 X-ray absorption spectroscopy

X-Ray Absorption Spectroscopy can be used to determine… (more than one answer is possible)

a) the presence of elements that occur in very low concentration

b) the chemical state of atoms in the sample

c) the transverse coherence of the X-ray beam

d) the doping of semiconductors

I.10.7.51 Ptychography

Ptychography… (more than one answer may be correct)

a) …allows to reconstruct the entire skeleton structure from a three-dimensional scan of the fossils of a Quetzalcoatlus Northropi (a pterosaur found in North America and one of the biggest known flying animals of all time)

b) …combines measurements taken from the same angle, but at different wavelengths

c) …requires precise positioning and rotation of the sample

$d)$ ... requires the rotation of the sample around three orthogonal axes

I.10.7.52 Undulator radiation

Derive the formula for the fundamental wavelength of undulator radiation emitted at a small angle θ:

$$\lambda = \frac{\lambda_u}{2\gamma^2}\left(1 + \frac{K^2}{2} + \gamma^2\theta^2\right)$$

from the condition of constructive interference of the radiation emitted by consecutive undulator periods!

I.10.7.53 Binding energies

In which atom are the core electrons most strongly bound to the nucleus?

$a)$ Neon

$b)$ Copper

$c)$ Lithium

$d)$ Osmium

$e)$ Helium

$f)$ Iron

$g)$ Sodium

$h)$ Gold

What about the valence electrons?

I.10.7.54 Electron and X-Ray diffraction

In comparison to diffractive imaging using electrons, X-ray diffraction...

$a)$... has the advantage that the sample does not need to be in vacuum

$b)$... gives a stronger diffraction signal for all crystal sizes

$c)$... generates the same signal for all atoms in the crystal

What are the consequences for the optimum sample thickness for electron diffraction in comparison to X-ray diffraction?

I.10.7.55 Practical applications of synchrotron radiation

The Italian Light Source Elettra is a 3rd generation synchrotron source with 259 m circumference, and can operate at beam energies of either 2.0 GeV or 2.4 GeV, with beam currents of 310 mA and 160 mA, respectively. The Machine Director is feeling thirsty, and would like to use Elettra to make a splendid espresso.

By assuming that all radiation emitted as SR from the dipole magnets can be converted into heat, calculate how much time is needed for the 2.0 GeV beam to heat up the espresso water from 20°C to 88°C. One espresso is 30 mL. The radius of curvature in the dipoles is 5.5 m. Neglect potential insertion devices!

Hint: the specific heat capacity of water is $c_w = 4.186 \frac{\mathrm{J}}{\mathrm{gK}}$.

References

[1] J.D. Jackson, *Classical electrodynamics*, 3rd ed. (New York, Wiley, 1999), pp. 237–294.

[2] Ph. Duke, *Synchrotron radiation: Production and properties* (Oxford, Oxford University Press, 2009).

[3] M. Sands, The physics of electron storage rings, SLAC-Report-121 (Stanford, Calif., 1970), https://www.slac.stanford.edu/pubs/slacreports/reports02/slac-r-121.pdf.

[4] A. Wolski, *Beam dynamics in high energy particle accelerators* (Singapore, World Scientific Publishing, 2023), doi:10.1142/13333.

[5] H. Braun *et al.*, SLS 2.0 storage ring. Technical design report, PSI Bericht Nr. 21-02 (Paul Scherrer Institute, Villigen, 2021), https://www.dora.lib4ri.ch/psi/islandora/object/psi:39635.

[6] A. Thompson *et al.*, X-ray data booklet, LBNL/PUB-490 Rev. 3 (Lawrence Berkeley National Laboratory, Calif., 2009), https://xdb.lbl.gov.

[7] C.P. Brock (ed.), International Union of Crystallography: International Tables for Crystallography, doi:10.1107/97809553602060000001.

[8] J. Beacham and F. Zimmermann, *New J. Phys.* **24** (2022) 023029, doi:10.1088/1367-2630/ac4921.